Paleohydrology repeating? Regional hydrological change may lead to an overflow and cross-mixing of an alkaline and freshwater lake in East Africa

Mathew Herrnegger[a], Pierre Kray[a], Gabriel Stecher[a], Nelly Cherono[b], Dennis Otieno[c], Luke Olang[b], Sharon E. Nicholson[d]

[a]Institute of Hydrology and Water Management, University of Natural Resources and Life Sciences (BOKU), Vienna, Austria

[b]Department of Biosystems and Environmental Engineering and Centre for Integrated Water Resources Management, Technical University of Kenya (TUK), Nairobi, Kenya

[c]Kampi Ya Samaki, Lake Baringo, Kenya

[d]Department of Earth, Ocean and Atmospheric Sciences, Florida State University, Tallahassee, FL, United States of America

Corresponding author: Mathew Herrnegger - mathew.herrnegger@boku.ac.at

Abstract

Study Region

Starting around 2010, several Rift Valley lakes of Kenya have experienced significant rises in water levels, thereby affecting nearly eighty thousand households of about 400,000 people.

Study Focus

There is presently fear of an ecological catastrophe, should the water levels of the alkaline Lake Bogoria continue to rise leading to an overflow and cross-mixing with the freshwater Lake Baringo, a hydrological situation witnessed around 8 000–10 000 years ago.

New Hydrological Insights for the Region

Over the past decade, the data reveal significant meteorological and hydrological changes in the study region. Average annual rainfall has more than doubled, with substantial increases in variability. Despite a decrease in the number of rainy days over the period, intense rainfall days have increased by +318%.

Relative to the maximum observed water level in 2020, a 0.7m increase in lake level would have been sufficient for Lake Bogoria to reach the sill point located at about 1000.2 m, beyond which an overflow into Lake Baringo begins to occur. In 2023, the lake level has declined by 1.5 m, resulting in a decreased risk of overflow to around 20%. Results indicate that mean annual rainfall after 2010 was high enough to provide an average annual flow of 500-1000 L/s from Lake Bogoria towards Baringo, if lake levels were at sill point elevation.

1 Introduction

Lakes are important water resource systems of the water cycle, contributing significantly towards regulation of the hydro-climatic conditions of an area and providing a wide range of ecosystem services for the local biodiversity (Hassan and Jin, 2014; Jenny et al., 2020). Across the globe however, there is evidence of degradation of the water resources system arising from various environmental stressors, classified largely as anthropogenic, climatic and to an extent, geological factors (Liu et al., 2023; Wu et al., 2022; Zadereev et al., 2020). Human-induced causes, primarily from various intensive and unregulated human interventions, are known to directly or indirectly affect the qualities and ecology of concerned water systems with short to long term effects (Kast et al., 2021; Shams Ghahfarokhi and Moradian, 2023; Spears et al., 2022). In some regions, shifts in regional hydro-climatic patterns has been shown to contribute to lake water level fluctuations, leading to short-term decreases or increases of volumes over the climatic periods (Hassan et al., 2023; Herrnegger et al., 2021; Yao et al., 2018). Today, sufficient evidence from paleo-studies of many lakes across the globe indicate water bodies that either changed course, geometry or otherwise completely desiccated over geological time-scales. A review of the lacustrine deposits of some of the lakes that have changed status from their pre-Anthropocene status is available through lake sediment achieves (Jenny et al., 2020).

In the East African Great Rift Valley (Gregory, 1896; Suess, 1891; von Höhnel et al., 1891), several lakes have witnessed substantial water level increases since around 2010 (Avery, 2020; Herrnegger et al., 2021; Onywere et al., 2013). In Kenya, a majority of the Rift Valley lakes are biodiverse eco-zones, classified as RAMSAR wetlands of international importance (Ramsar Convention, 2022), and UNESCO World Heritage Sites (UNESCO World Heritage Convention, 2023). The water level increases of the Kenyan lakes not only affect the biodiversity, but also inundated the basis of rural livelihoods and existing social amenities such as schools, hospitals, national parks or agricultural land. Consequently, up to eighty thousand households with about 400,000 people have been affected by the inundations (Government of Kenya and UNDP, 2021; Obando et al., 2016; Tower and Plano, 2023).

Herrnegger et al. (2021) presented evidence that changes in rainfall and evapotranspiration characteristics – the major hydro-climatic drivers defining the water balance of the lakes – has with high confidence resulted in the lake water level increases. In the period 2010–2020 the study shows that mean annual rainfall increased by up to 30% for the different lake catchments. After 2018, annual catchment rainfall increased by even more than 50%.

Regional climate in Eastern Africa has shown exceptional variability in the past, fluctuating between long-lasting periods of severe drought and wetter periods as we are currently observing (e.g. Bessems et al., 2008; Flohn, 1987; Nicholson, 2001, 2019; Nicholson et al., 2022; Nicholson and Yin, 2001; Sutcliffe and Parks, 1999; Verschuren et al., 2000; Whittaker, 2019). The existing scientific literature on the historic and paleo-climatic water levels, ranging back 30 000 years, comprehensively indicate that climate variability over the same region has led to not only complete desiccation of some lakes, but also high water stands in the historical past (e.g. Bessems et al., 2008; Dommain et al., 2022; Flohn, 1987; Garcin et al., 2009; Nicholson, 1998; Nicholson and Yin, 2001; Okech et al., 2019; Olaka et al., 2010; Owen and Renaut, 1986; Pavitt, 2008; Petek, 2018; Robakiewicz et al., 2023; Stager et al., 2005; Tiercelin and et al., 1987; Trauth and Strecker, 2019; Verschuren, 2019, 2001; Verschuren et al., 2000; Whittaker, 2019; Whittaker and Johnson, 2019; Wuytack et al., 2017).

Lake Naivasha in Kenya, for instance, was reduced to a puddle around 1850, which was a period of widespread and extreme aridity throughout most of Africa and certainly seen in other East African lakes. Also, particularly low levels persisted throughout the 1940s and 1950s. (Nicholson, 1998; Richardson, 1966; Trauth and Strecker, 2019). Pavitt (2008) (Figure 1) quoted that "*Three years of drought in the mid-1890s followed a decade of below-average rainfall and caused Lake Naivasha to virtually dry up. […]. The Maasai could drive their cattle straight across the 'lake'. By 1900 exceptionally heavy rain began to restore the level of the lake. […].*". This visual evidence is somewhat supported by reconstructions of Naivasha lake levels in scientific literature (Verschuren, 2001). In 2020, high stands in the water levels of Lake Naivasha, which is today a popular destination for leisure seekers from the capital city of Nairobi, led to flooding of built-up areas, farms, lodges, camp sites and protected areas.

Figure 1: Three years of drought in the mid-1890s followed a decade of below-average rainfall and caused Lake Naivasha to virtually dry up. This rare picture of the 'lake' with two Maasai warriors and Mount Longonot in the distance must have been taken in the closing years of the nineteenth century. The Maasai could drive their cattle straight across the 'lake' at the time. (source Pavitt (2008))

In the Rift Valley of Kenya, studies have documented extreme high stands of water levels historically witnessed by the lakes in the period between 8 000-12 000 years ago, when the area exhibited a completely different hydrological and river network pattern as compared to today. Lake Turkana (Avery and Tebbs, 2018; Ojwang et al., 2016), now one of the largest desert lakes in the world, drained towards the Nile. Lake Turkana – former Lake Rudolf – now receiving most of its water from Ethiopia via the Omo River, was part of a river system having its headwaters in today's Lake Elementaita area. The catchment boundaries were very different, not only for Lake Turkana (Dommain et al., 2022; Garcin et al., 2009).

For Lake Baringo, after Lake Turkana the second largest lake in the Kenyan Eastern Rift, Okech et al. (2019) provide information on water level dynamics from 1790 to 2014 based on sediment core samples and the abundance for planktonic and benthic diatom taxa and P/B ratio as a proxy. Information provided by Bessems et al. (2008) also indicate that most recent complete desiccation episode of Lake Baringo occurred in the late 18th and early 19th century; a complete opposite of what is being observed today. Late Pleistocene-Holocene reconstructions of water levels in Lakes Baringo and Bogoria show that the two lakes were connected around 8000 years ago (Ashley et al., 2004; de Cort et al., 2018; Dommain et al., 2022; Garcin et al., 2009; Tiercelin and et al., 1987; Wuytack et al., 2017).

Today, the increases in lake levels of Lake Bogoria may lead to a repetition of the paleohydrological conditions. There is fear of an ecological catastrophe, should the current water levels of the alkaline Lake Bogoria continue to rise. The result would be an overflow and mixing with the freshwater Lake Baringo, the basis of the local community supporting agriculture, tourism, and fisheries, but also the very basic need of drinking water (Avery, 2020; Muita et al., 2021; The EastAfrican, 2014; Wambui et al., 2021). Using data from the year 2020 (Facebook Connectivity Lab and Center for International Earth Science Information Network - CIESIN - Columbia University, 2016; Tiecke et al., 2017) our estimates suggest that 6,000–25,000 people would be affected. The large range underlines the uncertainties and depends on the area considered to be affected.

Although the current lake level rises in Kenya have received some attention in scientific literature (see references in Herrnegger et al., 2021 or Kiage and Douglas, 2020; Kimaru et al., 2019; Muita et al., 2021; Onywere et al., 2013; Walumona et al., 2022), no analysis exists to understand the potential overflow of Lake Bogoria and cross-mixing with Lake Baringo. There is currently a lack of analysis regarding the topographical and landscape conditions in the Loboi plain, situated between the two lakes, and the potential flow paths that might emerge in the

event of an overflow. The risk and extent of water level increases required for Lake Bogoria to reach its sill point remains uncertain. Also unclear are the climatic rainfall conditions, which are necessary to lead to sustained flows from Lake Bogoria towards Baringo.

Considering these constraints, this study seeks to assess:

(i) the rainfall conditions in the proximity of the lakes,
(ii) the overflow or sill point location and potential flow paths towards Lake Baringo,
(iii) the required lake water level and volume changes, until the sill point is reached and
(iv) the mean rainfall conditions, which would be necessary to provide the required volume and a sustained flow towards Lake Baringo.

The analysis is based on a comprehensive hydrological and topographical mapping of the area. To achieve this, we utilize remotely sensed data in conjunction with ground-based measurements, including station data and electrical conductivity as a proxy-tracer. Additionally, we integrate highly detailed topographical and elevation information from drone-based surveys, specifically focusing on the sill point area.

Satellite-based measurements and estimates of precipitation, lake levels, areas, and lake volume variations are used to infer properties and changes of the regional hydrological cycle, including trends in rainfall and the partitioning of rainfall and evapotranspiration. The analysis is further strengthened by the inclusion of in-situ data, supporting our assessment of rainfall trends.

Our investigation also focusses on the potential overflow of Lake Bogoria, encompassing the assessment of possible downstream flow paths as well as the risk of overflow occurrences. To establish a comprehensive picture, we draw upon 37 years of climate data spanning from 1984 to 2020, and 40 years of lake level data ranging from 1984 to 2023.

The findings are discussed, also in the context of uncertainties or paleo-hydrometeorological conditions. This work finally ends with a summary and conclusions derived from the results.

2 Materials and methods

2.1 General characteristics of the study area

Lake Bogoria and Baringo are located in the Central Rift Valley of Kenya, which is part of the East African Rift System, ranging from the Gulf of Aden at the Horn of Africa to the south of Lake Malawi between Malawi and Mozambique (Figure 2). In total, the study area and lake basins cover an area of 7,615 km². Lake characteristics are summarized in Table 1.

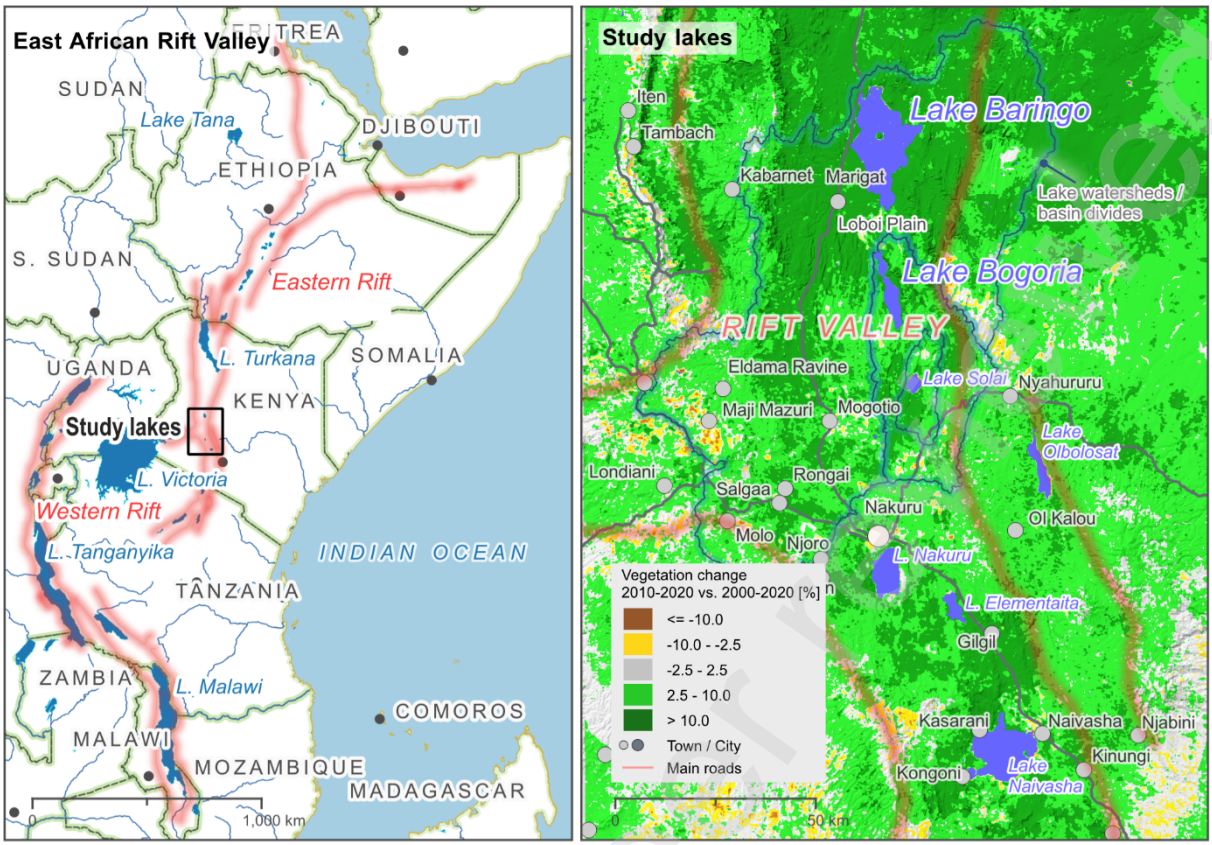

Sources: Global Surface Water (Pekel et al. (2016); Hillshade: SRTM (Jarvis et al. 2008); NDVI: MODIS MOD13Q1 (Didan, 2015); Lakes, rivers, towns, OpenStreetMap & NaturalEarth data; Roads: GRIP globals roads

Figure 2: Location of the study lake in the East African Rift Valley (left); Lakes in the central Rift Valley of Kenya, including study lakes and lake watersheds in the northern part of the Rift. In the background, the vegetation change between 2010–2020 and 2000-2020 is shown using the Normalized Differential Vegetation Index (NDVI) as a proxy (right).

Table 1: Lake characteristics (Herrnegger et al. (2021))

Lake characteristics	Baringo	Bogoria
Orographic catchment area [km²]	6608.7	1060.0
Mean catchment elevation [m]	1721.6	1774.1
Range in catchment elevation [m]	963 - 3014	980 - 2872
Mean annual catchment rainfall (1981-2020) [mm]	1023.7	1036.1
Mean annual lake area (1984–2020) [km²]	146.3	34.9
Standard deviation of mean annual lake area (1984–2020) [% of mean]	±19.3%	±9.1%
Range in mean annual lake area (1984–2020) [km²]	118.3 - 197	31.4 - 41.2
Mean annual lake level (1984–2020) [m]	973.8	994.4
Range in mean annual lake level (1984–2020) [m]	971.4 - 979.6	993.1 - 998.1

Both lakes lie in closed basins, where the lake is a sink and where no obvious surface outlets are present. Lake Bogoria and Baringo are located in the Rift floor, encircled by high mountain ranges and escarpments. The lowest lake regarding lake level but also mean catchment elevation of 1722 m is Baringo, which is freshwater. Despite high potential evapotranspiration rates, Lake Baringo has not become saline, indicating that there is substantial underground loss of water through seepage, which hinders the accumulation of dissolved solids through flushing (Becht et al., 2006; Darling et al., 1996, 1990; Derakhshan, 2017; Yihdego and Becht, 2013). A potential emergence of Lake Baringo seepage waters could be the hot springs in Kapedo (1°10'47.52"N, 36°6'41.31"E), which lie about 50 km to the north. Bogoria is in contrast highly saline, which however does not mean that no underground seepage is present. The magnitude of underground seepage is low, compared to the freshwater lake (McCall, 2010).

Lake Baringo (Kiage and Douglas, 2020; Obando et al., 2016; Odada et al., 2006; Onywere et al., 2013) is internationally recognized for its biodiversity, but is also important to the communities in its basin as a source of water for domestic and agricultural use and watering livestock. Other important uses are income generation through tourism, biodiversity conservation and fishing. Three indigenous human communities live in the basin namely the Ilchamus, Pokots and Tugens. Seasonal rivers that drain into the Lake Baringo include Ol Arabel, Makutan, Tangulbei, Endao and Chemeron. Perkerra and Molo are perennial, but show strong seasonality with significantly lower discharges during dry season. Lake Baringo experiences very high annual evaporation rates (1650-2300 mm), compared to an annual rainfall of 450-900 mm and therefore lake levels depend heavily on inflows from rivers originating from the humid parts of the drainage basin, where the annual rainfall varies between 1100 mm and 2700 mm (Herrnegger et al., 2021; Onywere et al., 2013). Conductivity is reported to be around 1760 µS/cm (De Bock et al., 2009), 894.4 µS/cm (Obando et al., 2016) or 450-500 µS/cm (this study). The orographic catchment size of Lake Baringo is around 6610 km², having a north-south extent of around 150 km and 70 km from west to east. The area around Lake Baringo is presently inundated with several hotels and rural infrastructure, including homes, agricultural fields and grazing areas, dispensaries, health centres and schools being affected.

Lake Bogoria (see e.g. Agembe et al., 2016; McCall, 2010; Renaut et al., 2017; Tiercelin and et al., 1987) is located in a deep depression with comparatively steeper slopes than Lakes Baringo. Although the lake level increases, when measured in absolute number, are high, the steeper topography of the surrounding area limits the spread of flood waters mostly to the north of the lake. The lake is located within a National Reserve, where the main road, main gate and

administration building have been flooded. Geothermal springs associated with the lake region (Renaut et al., 2017) and a prominent touristic attraction have been submerged. The lake is highly alkaline, with reported conductivity of 31 046 µS/cm (Obando et al., 2016) and 33 800 µS/cm (this study). The catchment area is around 1060 km², receiving around mean annual rainfall of 1035 mm for the period 1981-2020.

2.2 Data Basis

The analysis builds on data with information on (a) elevation and topography, (b) lake levels, lake areas and lake volume variations, (c) electrical conductivity and temperature conditions, current extents of swamps, river courses and vegetation cover and (d) rainfall, runoff and water balance. Figure 3 provides an overview of all these data sets.

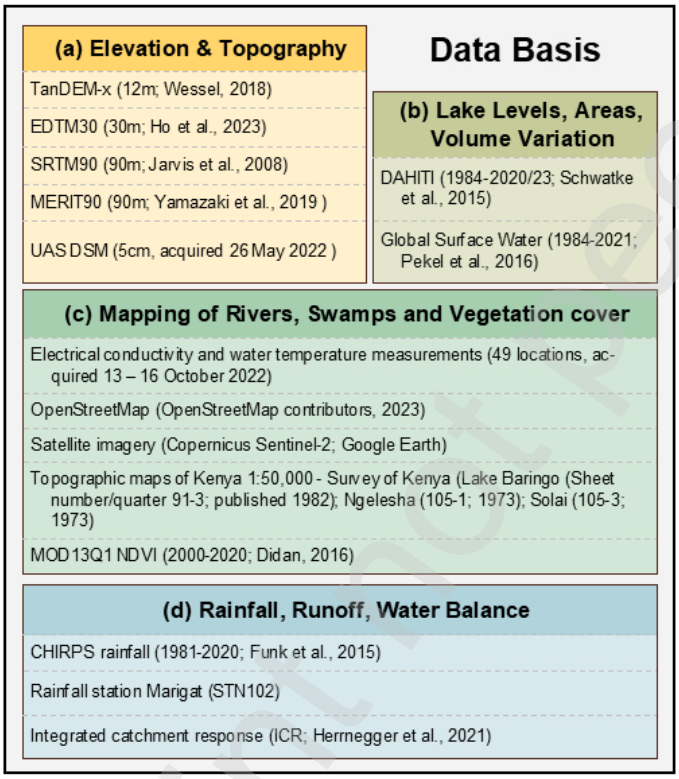

Figure 3: Overview of the data basis, incl. references

2.2.1 Elevation and Topography

Different elevation models (TanDEM-x (spatial resolution of 12m, Wessel, 2018); EDTM30 (30m, Ho et al., 2023), SRTM (90m, Jarvis et al., 2008), MERIT Hydro DEM (90m, Yamazaki et al., 2019), and a drone or Unmanned Aircraft System (UAS)-based elevation model with a 5 cm resolution are used for delineating watershed boundaries, extracting profiles, modelling shorelines and analyzing the sill point and potential flow paths. The TanDEM-x also builds the basis for the estimation of lake shores, water volumes and visualization of the region.

To take care of geoid undulations, corrections of some of the elevation data were performed to compensate for differences in vertical datum of the raster data. The horizontal and vertical datum of the TanDEM-x digital elevation model (DEM) is the World Geodetic System 1984 (WGS84) in G1150 realization (Rexer and Hirt, 2016). The same ellipsoidal vertical datum is present in the UAS DSM (Unmanned Aircraft System Digital Surface Model). In contrast, EDTM, SRTM and the MERIT use the World Geodetic System 1984 (WGS84) as horizontal datum and the Earth Gravitational Model (EGM96) geoid as vertical datum. Also due to its more popular distribution, elevations based on the Earth Gravitational Model used in EDTM30/SRTM/Merit are therefore also used in this study. The difference of absolute elevation values due to the different vertical datums of TanDEM- x/UAS DSM and EDTM30/SRTM/Merit lies around 14.4 m in the south of Lake Bogoria to around 15.1 m in the south of Lake Baringo, with values of around 15 m on the Loboi Plane. The geoid thereby is higher, compared to the TanDEM- x/UAS DSM. Figure A1 in the Appendix shows the spatial distribution of the geoid undulations used for the additive correction for the study area, which is an interpolated field based on 5 000 randomly sampled points, for which the geoid undulation was calculated using UNAVCO (2021).

The UAS-based DSM covers 392 ha of the location of the Bogoria sill point and was acquired on 26 May 2022. It was the second attempt to capture the elevation data after the first drone crashed into the lake southeast of the flooded former Loboi Health Clinic. Over a day was unsuccessfully spent searching for the drone and the data after the misfortune. All flights were performed following best practice guidelines (e.g. Strelnikova et al., 2022), using a stationary Differential Global Positioning System (DGPS) station for spatial reference improvements. Processing of the RGB images and deriving the DSM was performed using AgiSoft (AgiSoft, 2016).

2.2.2 Lake levels, areas and volume variation

Lake levels, areas, and volume variation data for Lake Baringo and Bogoria from the “Database for Hydrological Time Series over Inland Waters” (DAHITI, Schwatke et al. (2020, 2019, 2015) are used and are partially based on the data and results processed in Herrnegger et al. (2021), covering the years 1984–2020. Additional DAHITI water level data ranging until June 2023 was provided for the study. Furthermore, maximum water extents from the Global Surface Water product (GSW 1.1; (Pekel et al., 2016) are used as additional reference regarding water surfaces.

2.2.3 Information and mapping of river courses, swamps, and vegetation cover

2.3 A field campaign in October 2022 provided information on the electrical conductivity and temperature characteristics of 49 locations (Tables

Table A1), starting in the headwaters of the Molo and covering the different tributaries to Lake Bogoria and Baringo, but also the streams, swamps and other water bodies in the area between the lakes (Loboi Plain). A WTW cond315i conductivity meter was used to do the measurements, having accuracies of ±0.5% for electrical conductivity and ±0.1°C for water temperature.

Topographic maps of Kenya with a scale of 1:50.000 (Lake Baringo (sheet number - quarter 91- 3; published 1982); Ngelesha (105-1; 1973); Solai (105-3; published 1973) of the Survey of Kenya proved to be valuable for orientation and mapping and assurance of the current situation in the Loboi Plain. The swamps and river courses are based on OpenStreetMap (OpenStreetMap contributors, 2023) and were downloaded using the QuickOSM plugin in QGIS (QGIS Development Team, 2023). Additionally, river courses and water areas and extents were manually checked for plausibility via satellite imagery using Copernicus Sentinel-2 data and Google Earth Pro. Information on vegetation cover and spatio-temporal change (see Figure 2) based on the Normalized Difference Vegetation Index (NDVI) was derived using the MODIS MOD13Q1 product (Didan, 2015), using R (R Core Team, 2023) and different packages therein for processing, e.g. Busetto and Ranghetti (2016).

2.3.1 Rainfall, runoff and water balance

Climate Hazards Group InfraRed Precipitation with Station data (CHIRPS (Funk et al., 2015)) and in-situ rainfall information from station data measured at Marigat (STN102) in the proximity of the lakes is used as rainfall input.

Although some discharge data is at our disposal, the frequent data gaps and partially questionable data integrity hinders the use of this data for analyzing the water balance. The Integrated Catchment Response (ICR [mm]) from Herrnegger et al. (2021) provides information on fluxes of the lakes. The ICR is basically the integral runoff depth of *all* flows resulting in a change of water volume. It is solely based on changes in lake volumes and therefore integrates and includes all fluxes to and from the lakes, also including runoff to the lake, rainfall and evapotranspiration from the lake surface or potential groundwater flows. The ICR reflects a mean watershed or catchment value of the runoff coefficient, thereby averaging out spatial variability of hydrological processes e.g. of rainfall of evapotranspiration. We use the long time series of the ICR, which is calculated using lake volume variation data from 1984–

2020, for estimating the hydrological conditions influencing the lake levels. No quantitative information is available on groundwater flows towards the lakes.

2.4 Estimation of sill point location and potential flow path

The derivation of the sill point location is based on terrain analysis using QGIS (QGIS Development Team, 2023) utilizing the different DEMs available for the area of interest. For finding the location of the sill point, a catchment delineation is performed for the locality. The lowest point in the catchment divide between Lake Bogoria and Lake Baringo can then be defined as the sill point. Field work in February and October 2022 was essential for plausibility checks of the results.

The derivation of the potential flow path of the Bogoria-Baringo stream is based on a stream network delineation as a first guess, followed by the analysis of water courses depicted in the 1:50 000 scale topographical maps of the study area and GIS data on swamps and water courses from OpenStreetMap (Kray, 2023). Satellite imagery and additionally, field work and electrical conductivity measurements used as a proxy for understanding the current flow conditions, are used to check plausibility of the delineated water course.

Finally, after deriving the sill point and the potential water course, an elevation profile was generated by sampling mean elevation values from different elevation models (TanDEM-x, EDTM30, SRTM, UAS DSM) along the potential water course.

2.5 Necessary lake level and volume changes until sill point elevation is reached

The estimation of the necessary water level and volume changes of Lake Bogoria until the sill point is reached is based on the elevation of the Bogoria sill point and the maximum water level present in the DAHITI database. The differences in the water levels of these two states (maximum observed water level and sill point water level) yield the necessary lake level increase until the sill point is reached. For additional evaluation, the water levels at the time of writing of the first half of 2023 are also used as reference.

The elevation contour line of the sill point elevation is used to model the water surface of Lake Bogoria, which would occur, if the water level would reach the sill point. For the area of the sill point, the DEM derived from the UAS-data was integrated into the TanDEM- x, since we have higher confidence in these elevation values. Subtracting the two water surfaces of the maximum water level (and the water level of the February 2023) from the sill point water surface yields the water depth for every grid cell. This information has a spatial resolution of 12 m, since we used the TanDEM-x as basis. Considering the grid cell size and water depth, a

volume can be calculated for every grid cell. These volumes can then be integrated to receive the total volume change.

A reconstruction of the water surface at the maximum water level of DAHITI was also necessary, since plausibility checks showed that the water areas included in DAHITI substantially underestimated the real water areas. This is the case for Lake Bogoria, but also Lake Baringo. This underestimation is also present, when comparing DAHITI water areas with delineations available in Government of Kenya and UNDP (2021) and Onywere et al. (2013) and is also discussed and shown in Herrnegger et al. (2021; see e.g. Fig. A6 and Fig. A7 therein).

To assess the risk of an overflow of Lake Bogoria, we use historical lake level data as a proxy. These lake level fluctuation data are used to calculate the empirical probability of water levels to reach the sill point. We estimate the likelihood that the sill point is reached, assuming that the temporal sequence of observed lake level rises but also declines follow comparable patterns as in 39 years of water level data.

2.6 Mean rainfall conditions to provide a sustained flow towards Lake Baringo

Understanding the underlying mechanisms leading to the lake level fluctuations necessitate an analysis of the temporal characteristics of the water balance and inflows to the lakes. Bringing the volume term to the left, the following longer-term water balance equation for a *lake watershed* can be defined (all units in [mm]):

$$V = R + Q_{gw} - AET - Q_{out} + \Delta S \quad (2)$$

where V refers to storage or volume in the lake (i.e. increase/decrease in lake water volume from one year to the next), R to catchment rainfall, Q_{gw} to additional potential underground flow from neighbouring watersheds, AET to the actual catchment evapotranspiration (including evaporation from the lake surface), Q_{out} to runoff from the lake (i.e. outflow through a surface water body or the seepage into the underground) and finally ΔS to changes in storage in the catchment (e.g. change in soil moisture, groundwater or water stored in biomass).

The lake volume variation data from DAHITI can be interpreted as the right-hand side of Eq. (2) since V integrates potential changes occurring in the catchment. It allows to quantify the magnitude of changes to be expected on the right-hand side of the water balance equation. The year-to-year lake volume variation data is, in combination with orographic catchment area, used to derive a magnitude for every year t, which we refer to as "Integrated Catchment Response" (ICR, mm):

$$ICR_t = \frac{\left(S_t[\mathrm{km}^3] - S_{t-1}[\mathrm{km}^3]\right) * 10^{12}}{\mathrm{Area}[\mathrm{km}^2] * 10^6}\,[\mathrm{mm}] \quad (3)$$

In Eq. (3), the difference in lake volume variation S from one year to the next is calculated and converted from [km³] to [dm³] and is then normalized by the orographic catchment area (Area), which is converted from [km²] to [m²]. This results in the unit [mm] for the ICR.

Substituting the lake volume V in Eq. (2) with the ICR and assuming an equilibrium between Q_{gw} and Q_{out}, so that these two terms cancel each other out, and assuming that the storage term ΔS can be ignored on a longer-term time scale, the following equation can be formulated:

$$AET_t = R_t - ICR_t \quad (4)$$

Then the ratio between actual evapotranspiration and rainfall of the catchment ($r_{AET/R}$) can be calculated, which we use to better understand the catchment water balance and partitioning of rainfall and evapotranspiration:

$$r_{AET/R} = \frac{AET_t}{R_t} \quad (5)$$

Given the case that Lake Bogoria water level has reached the sill point, it is assumed that further (excess) inflow will lead to a sustained flow towards Lake Baringo. The question is, which catchment rainfall values are necessary, so that the flow can be sustained. For this, we establish a relationship between the observed Integrated Catchment Response (ICR) and catchment rainfall to provide a transfer function to simulate necessary rainfall conditions for different sustained flow scenarios. For the evaluation, different flow scenarios ranging from 10 L/s to 1500 L/s are considered.

3 Results

3.1 Water-related characteristics of the Loboi Plain

Figure 2 provides a general overview of the Loboi plain and situation between Lake Bogoria in the south and Lake Baringo in the north. The map depicts the minimum and maximum lake water surfaces between 1984 and 2020. The maximum water level thereby occurred in November 2020. Anticipating the results, the map also shows the contour lines of the elevation of the sill points of Lake Bogoria and Baringo and the potential flow path of the water course between the two lakes.

To the south-east of Baringo the courses of the perennial Perkerra and Molo rivers, the main water sources of Baringo, are visible. Both are extensively used for irrigation in the Loboi plain

and are essential lifelines in the semi-arid area. The Molo flows into the Ng'arua Swamp, the Perkerra ends in the Oloimatashu swamp, which is currently mostly submerged and part of Lake Baringo. Just west of Lake Bogoria, the Loboi River is visible. It is to our knowledge perennial, having its permanent source in Maji Moto hot springs, around 10 km south of the northern end of Lake Bogoria. The catchment of the Loboi River however extends much further to the south. The Loboi River flows into the Loboi Swamp and is also used for irrigation. The diversions made for irrigation purposes divert water towards the Kiborkoch Swamp (see panel (b) in Figure 2). East of Lake Bogoria, the Waseges or Sandai River emerges through an impressive canyon in the village of Sandai. Although the flows are seasonal, water from the river is diverted for an extensive irrigation scheme.

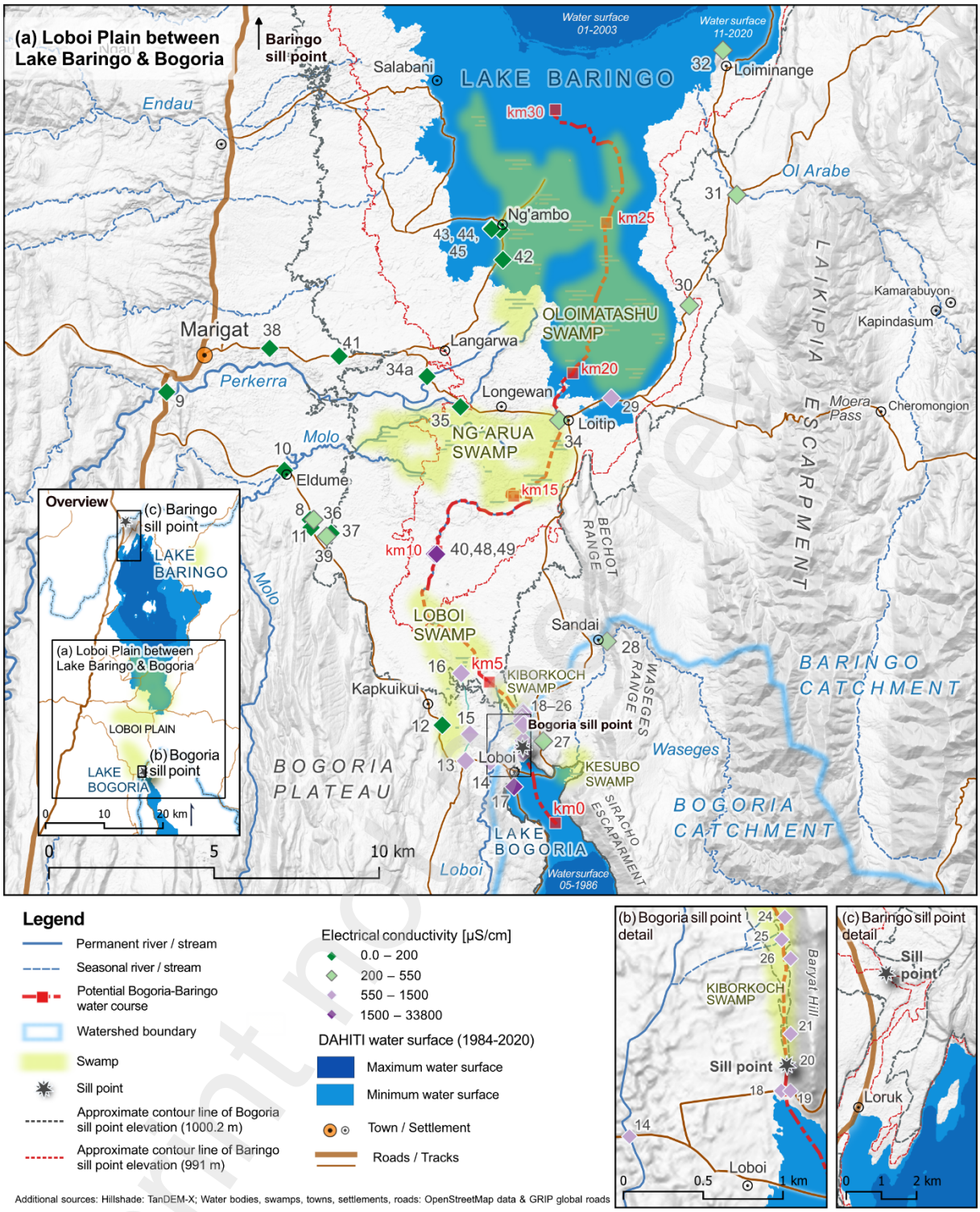

Figure 4: Maps showing different aspects and details of the study area: The small overview map shows an overview of the area under investigation, including the extents of maps (a)-(c), swamps, watershed boundaries and roads. (a) shows the Loboi Plain between Lakes Baringo and Bogoria, incl. location of electrical conductivity measurements, Bogoria sill point and approximate elevation contours for Bogoria and Baringo spill points. (b) and (c) show details of the spill points.

Figure 2 also shows a spatial overview of the electrical conductivity (EC) of the surface water bodies. The tabulated values, including water temperature values, are available in the Appendix. In the southwest, where the water sources are Perkerra and Molo, lower EC values mostly in the range of 130-200 µS/cm are present. In contrast, the EC values in the southeast around Lake

Bogoria lie in the range of 550-1500 µS/cm. The Loboi river, for example, showed an EC value of 1042 µS/cm. The highest EC value of 33 800 µS/cm was measured at Lake Bogoria (Number 17 in Figure 2).

EC measurements at the Loboi stream between the Loboi and Ng'arua swamps showed surprising high values of around 1600 µS/cm (number 40, 48 and 49 in Figure 2). The very small stream had a flow of only a few litres per second and was very turbid. The high EC values do not fit into the larger picture, since the Loboi flowing towards the Loboi Swamp from the south showed lower EC values of around 1000 µS/cm and waters from the hot springs at the Lake Bogoria Spa Resort also feeding the swamp showed values of approximately 650 µS/cm. The reason for the high EC values is at this time speculative and may be a result of accumulation of salts due to strong evaporation in the Loboi Swamp, contributing (underground) flows from Lake Bogoria or strong activation of sediments due to cattle watering.

3.2 Rainfall conditions since the lake level rises 2010

Marigat, to the west of the Loboi plain, is the main town and trading center in the region. Marigat received 463 mm of mean annual rainfall in 1986-2009. Although this value increased to 978 mm for the period 2010-2018 (corresponding to +111%), the number of days with rainfall has decreased by 19% (Table 2; Figure 5). Also corresponding to the impression of the local people (Petek-Sargeant, 2023), the days with intense rainfall has increased by nearly 320% in the last decade, an astonishing value (Table 2; Figure 6). The division of the time series is based on the finding from Herrnegger et al. (2021), who show that 2009 was a breakpoint year, where the means and structure of the catchment rainfall time series have changed. The tabulated values of annual rainfall are documented in Table A2 in the Appendix.

Table 2: Rainfall climatology and characteristics for Marigat (STN102)

	Rainfall Marigat (STN102)					
Period	Mean annual rainfall [mm]	Deviation from 1986-2009 [%]	Annual days with rainfall ≥0.1 mm/d	Dev. from 1986-2009 [%]	Annual days with rainfall ≥30 mm/d	Dev. from 1986-2009 [%]
1986–2018	603	30%	59.9	-10%	4.7	86%
1986–2009	463	0%	66.3	0%	2.5	0%
2010–2018	978	111%	53.4	-19%	10.4	318%

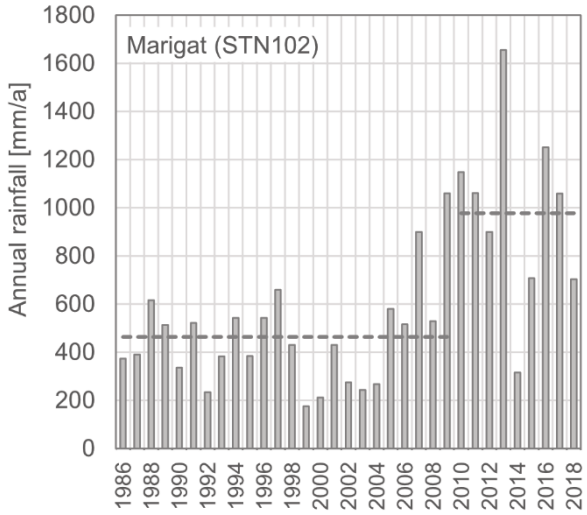

Figure 5: Annual rainfall sums for Marigat. Before the lake level rises, the average annual rainfall in Marigat was 463 mm/a. After 2010, the mean increased to 978 mm/a or +111%. The dashed lines show long-term averages of 1986– 2009 and 2010–2018.

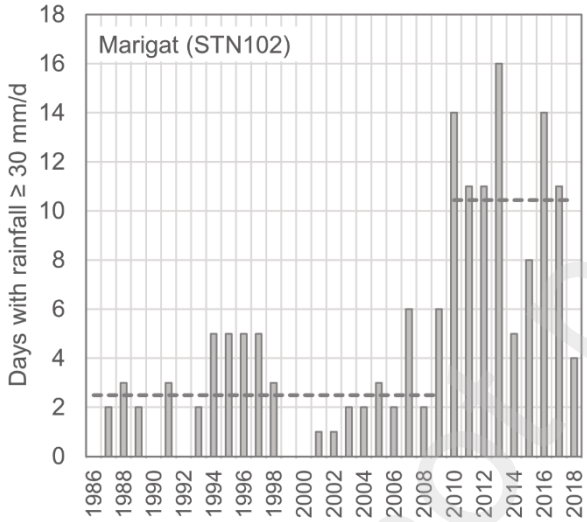

Figure 6: Number of days per year with intense rainfall using 30mm/d as threshold. Although the number of days with rainfall decreased by around 20% between 1986-2009 and 2010-2018, the days with intense rainfall increased by nearly 320%. The dashed lines show long-term averages of 1986– 2009 and 2010–2018.

The seasonality of rainfall measured by the mean monthly rainfall shows an increase in rainfall in all months, except February (Figure 7). Largest increases in the means, at least on relative terms, are found for the months July, August and September, with increases of 517%, 208% and 291%, when comparing mean monthly rainfall 1986-2009 and 2010-2018.

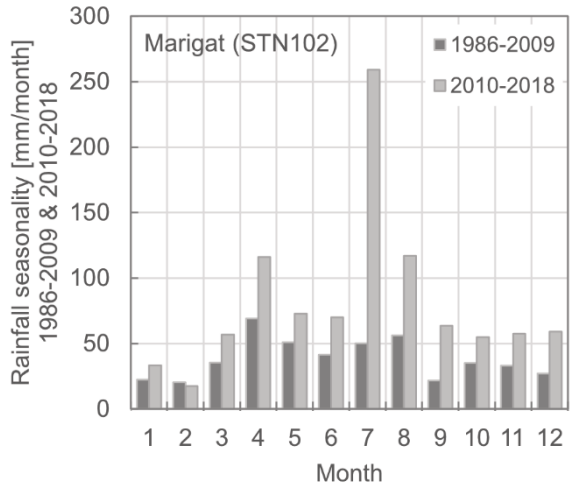

Figure 7: Mean monthly rainfall sums [mm/month] for Marigat for 1986-2009 and 2010-2018

People in the area report that the seasonality in rainfall - essential for planning agricultural decisions, e.g., when to plow or the definition of sowing dates - has become erratic and difficult to trust. This is also supported by the analysis of the Marigat rainfall data. Figure 8 show the monthly rainfall variability measured by the standard deviation for 1986-2009 and 2010-2018 and compared to the long-term values of 1986-2018. The standard deviation is thereby calculated for every single month. From the plot it is evident that the monthly rainfall variability has increased very strongly. Like the mean monthly rainfall, highest increases in variability are found for July, August and September, with increases of 455%, 236% and 246%. On average and for all months, the variability has increased by 200%, an impressive value and supports the impressions of the local people.

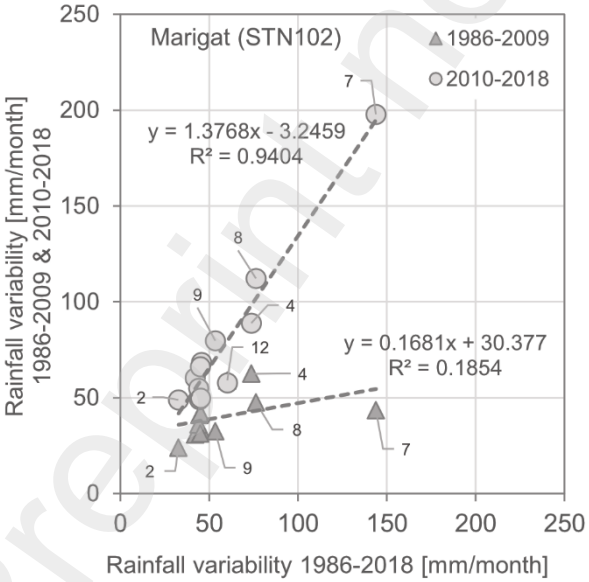

Figure 8: Monthly rainfall variability measured by the standard deviation for 1986-2009 and 2010-2018 and compared to the long-term values of 1986-2018 shown on the x-axis. Every point refers to a month, whereas some months are labelled.

These brief analyses for Marigat, located at the edge of the Loboi plain, show substantial changes in the rainfall quantity and temporal distribution since 2010. Mean annual rainfall has more than doubled, the variability has also substantially increased making planning based on the well-known rainfall seasons more difficult. The findings are in line with the results presented in Herrnegger et al. (2021), although (i) magnitudes differ and (ii) different time periods and (iii) footprints (i.e. point data here vs. catchment averages) are compared. Compared to the catchment averages, the point data show a much more pronounced change signal, e.g. in rainfall increases. For example, catchment averages for the Baringo catchment covering an area of around 6 800 km², increased by around 30% compared to 111% for the point measurement at Marigat. This is not surprising and can be explained by the phenomenon that averages for a larger area will always be smoother, since extremes at single locations tend to average out each other.

3.3 Sill point location and potential water course

The sill point of Lake Bogoria is located around 150-250 m north of Lake Bogoria and the new Loboi-Sandai road, which was constructed after the old road passing further south was flooded (Figure 9). The lake shore reached the dam of the new road during the observed maximum water level. Based on DAHITI, the lake level reached 999.5 m in November 2020. This maximum water extent shown in Figure 9 was reconstructed based on the DAHITI water level corrected for geoid undulations. The DAHITI water extent data for that time is biased due to misclassification of rather shallow water and poor image quality. It was therefore not used.

The sill points were derived from different Digital Elevation Models (DEMs), first calculating the watershed divides and then assuming the sill point to be the lowest point along the ridges.

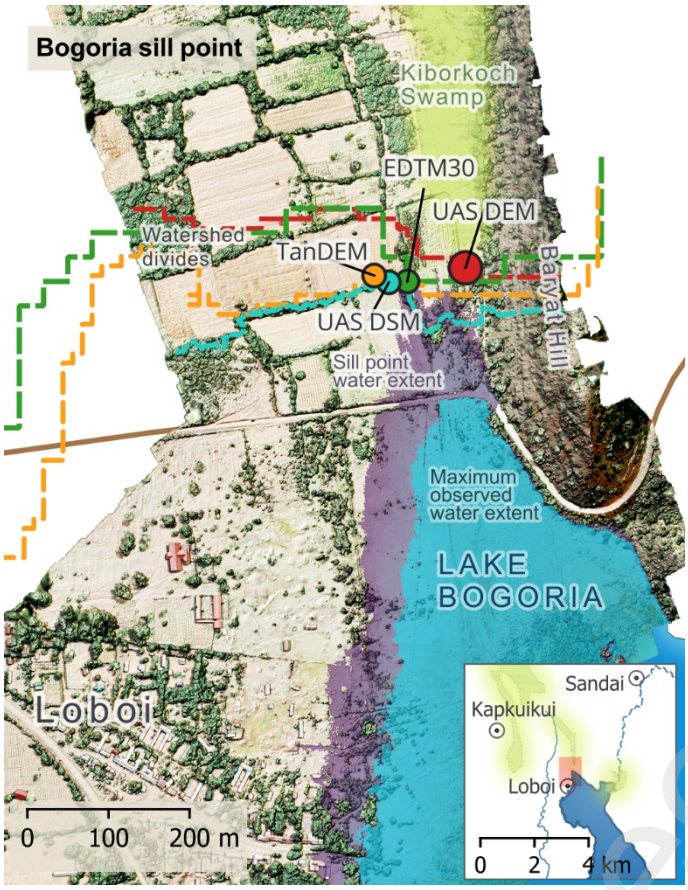

Figure 9: Detail of sill point location in the north of Lake Bogoria showing the UAS-based areal image and terrain in the background. Shown are sill points derived from different digital elevation models, namely TanDEM-x, EDTM30 and a UAS-based digital surface (UAS DSM) and elevation model (UAS DEM). For the UAS DEM trees and vegetation were removed to represent the terrain, leading to the most realistic sill point. Also visualized are the maximum observed water extent (November2020) and the simulated water extent in case the lake rises to the sill point.

The sill point based on the UAS-based Digital Surface Model (UAS DSM) is close to the TanDEM-x (12 m resolution) and EDTM30 (30 m) estimates. This is the case, although the high-resolution UAS-data has 57 600 (360 000) more information points - per raster or pixel - compared to the 12 m (30 m) satellite-borne data sets.

Trees and vegetation clearly influence the local topographical situation. This is also very evident in the high resolution 5 cm UAS-based Digital Surface Model (UAS DSM) and partially explains the proximity of the three estimates. When filtering and attempting to remove trees and vegetation from the Digital Surface Model and deriving a DEM (UAS DEM) applying *RemoveOffTerrainObjects* from the WhiteBox Tools (Lindsay, 2023), the estimated sill point moves around 90m to the east to the foot of the Baryat Hill, which is around 100 m high, compared to the surrounding terrain. The estimated location of the UAS DEM is the most realistic estimate and corresponds to our observations in the field.

Figure 10 shows the elevation profile for the potential water course between Lake Bogoria and Baringo. The water course and chainage is also depicted in the map of the study area in Figure

4. The elevation profile also shows the minimum and maximum water level in Lake Bogoria and Baringo based on DAHITI for 1984–2020, as well as approximate locations of the different swamps in the area and through which the water course would probably flow.

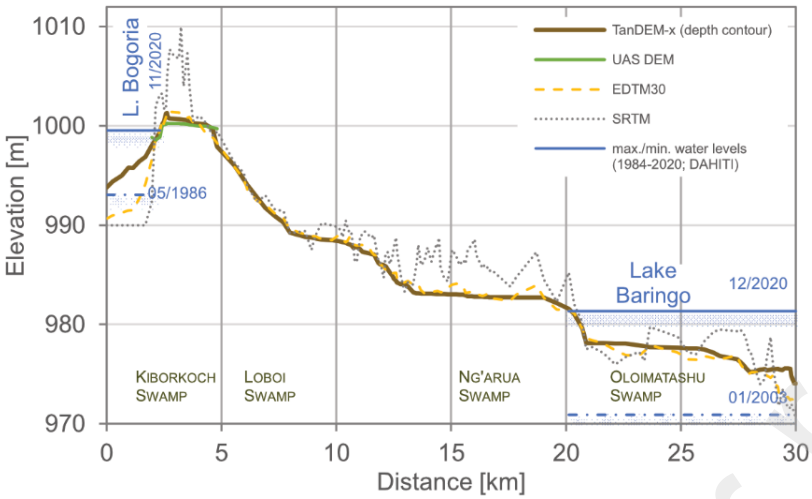

Figure 10: Elevation profile for the potential water course between Lake Bogoria and Baringo shown in Figure 4 and which is evaluated for different elevation models. The distance shown on the x-axis corresponds to the chainage also shown in the map of the study area. The sill point is located at km 2.6.

The Kiborkoch swamp is located at the foot of the Baryat Hill north of Lake Bogoria and stretches towards the north. The swamp is also mentioned in Wambui et al. (2021), however with a name, which could not be verified by the local people. This swamp generally exhibits a very minor gradient towards Lake Baringo and can be seen as a sill point swamp and the origin of a bifurcating stream. Figure A2 in the Appendix provides a visual impression of swamp in the proximity of the sill point. Due to the small gradients, water will also flow towards the south and Lake Bogoria, if water levels in the swamp are high enough. This was the case during our field visit in October 2022, when a minor flow was present towards the south. The origin of the water in the Kiborkoch swamp was irrigation water diverted from the Loboi river. Similar electrical conductivity values of the two waters of around 1000 µS/cm, but also flow paths visible in the drone images support this hypothesis (see also spatial distribution of EC values in Figure 4).

The potential water course would transvers the Kiborkoch Swamp, followed by the Loboi Swamp, which has a much higher gradient, also compared to the following Ng'arua and the currently mostly submerged Oloimatashu Swamp. In the Loboi Swamp, the potential water course would join and follow the channels already present leading to Lake Baringo (Figure 4).

The length of the potential water course, using the maximum water extents of Lake Bogoria and Baringo in 2020 as reference, is around 17.5 km. When the two lakes showed minimum

water levels, the length of the potential water course would have been nearly double that values, namely 33.2km.

The general picture regarding the elevation profile and gradients shown in Figure 10 is similar for all evaluated elevation models. Very prominent however are larger deviations and spikes of the SRTM compared to the other DEMs. One reason is the coarser resolution of the SRTM of 90m. This leads to a biased elevation around the sill point area since the 100 m high Baryat Hill next to the Kiborkoch swamp is somewhat reflected in the average grid cell values. Further downstream, between km 10 and km 20, the larger deviations of around 5 m in elevation can be explained by trees and vegetation, which surround the Molo River and which the potential water course would follow.

3.4 Required lake water levels and volume changes, until the sill point is reached

The previously shown elevation profile illustrates that the maximum water levels in Lake Bogoria in November 2020 were very close to the sill point elevation. Compared to the maximum water level of 999.5 m observed by satellite altimetry, only 70 cm additional water level or 0.033 km³ additional lake volume would have been necessary, until the lake reaches the sill point.

Table 3 shows the sill point elevation for the different elevation models and the necessary water level and lake volume increases, until the sill point is reached. As described in the previous section, the numbers found from the UAS DEM seem to be the most realistic estimate. For visual impression of the situation, the reader is referred to Figure 9, which also illustrates the water extents for lake level 999.5 m and the sill point elevation.

*Table 3: Sill point elevation derived from the different elevation models. Also shown is the elevation difference ΔH to the maximum water level observed at Lake Bogoria in November 2020 (999.5 m) and the additional lake water volume ΔV until the sill point would be reached. The results from the UAS DEM are highlighted in bold, since they closely match our observations in the field and are used for further analyis. *The ΔV for the UAS DEM includes data of TanDEM, since the UAS data only covers a small portion of the lake.*

Elevation Model	Sill point elevation [m]	ΔH to maximum water level 999.5 [m]	ΔV to maximum water level 999.5 [km³]
TanDEM	1001.3	1.8	NA
EDTM30	1001.5	2.0	0.322
UAS DSM	1001.6	2.1	NA
UAS DEM	**1000.2**	**0.7**	**0.033***

Figure 11 shows the lake water levels for Bogoria from January 2009 to February 2023, including the annual averages and the sill point elevation of 1000.2 m. A plot on the lake volume variation data can be found in Figure A3 of the Appendix. The numerical values of annual lake levels and lake volume variation are documented in Table A3.

From 1984 - 2009 the DAHITI data shows a very low variability in lake water levels, ranging from 993.1 m to 994 m, with an average of 993.5 m and a range of only 0.7 m. From January 2009 to November 2020, lake levels rose from 993.8 m to 999.5 m, an increase of 5.7 m. It is also visible that the margin to the sill point elevation (dashed line in Figure 11) was only 0.7 m or 70 cm and thus quite small.

Figure 11 also shows that the lake level has fallen since the high stand and lie at 998 m in February 2023. At the time of writing, the last reported value from DAHITI for Bogoria was from 27 June 2023 with a water level of 997.9 m. Compared to the value of 998 m, the elevation difference to the sill point is now 2.2 m.

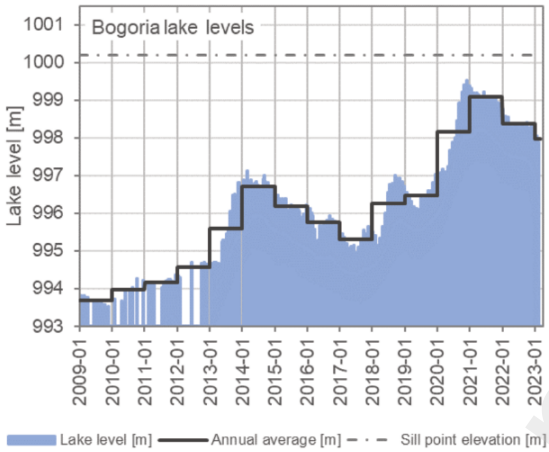

Figure 11: Bogoria lake levels, including annual averages and the sill point elevation of 1000.2 m. Information after the 29.03.2016 is based on satellite altimetry and was recalculated for this study. Lake level data before 29.03.2016 is based on hypsometry data.

Figure 12 (numerical values in Table A4) shows the year-to-year change in average annual water level, highlighting the low interannual variability before 2009. After 2009–2010, although year to year values of decreases exist between 2014 and 2016 and 2021–2022, lake levels mostly increased. Annual water level increases of around +1 m were frequent, with a maximum of +1.7 m from 2019 and 2020.

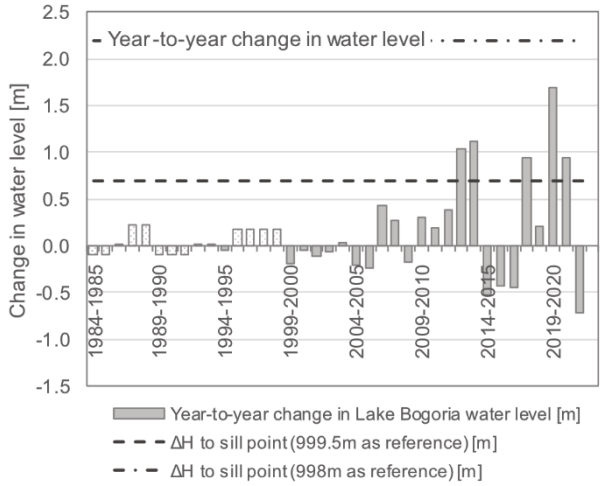

570

Figure 12: Year to year changes in average annual water level of Lake Bogoria. Horizontal lines show the necessary change in lake level until the sill point is reached, with 999.5 m (maximum observed water level; 0.7 m) and 998 m (water level in February 2023; 2.2 m) as reference. The dotted bars show years, where linear interpolation was necessary due to missing data.

575 The observed year to year changes in water level from Figure 12 are used to derive the empirical probabilities of Lake Bogoria to reach the sill point elevation, evaluated for the maximum observed water level in November 2020 (999.5 m) and water levels from February 2023 (998 m). Additionally, since the characteristics of lake level fluctuations differ before and after 2009, the empirical probability is also evaluated for the two climate conditions, namely the 580 long-term climate 1984–2022 and the wetter 2009–2022. The evaluation of the empirical probabilities solely relies on lake level fluctuations and does not include any other data. The empirical probabilities are assessed by computing the relative occurrence of the observed year to year water level changes to reach the sill point from both initial values (2.2 m - 2023, 0.7 m - 2020). The probabilities of reaching the sill point within 2 to 5 years are also assessed by 585 computing the relative occurrence within the according time periods, but instead of using the single year to year water level changes, the cumulative water level changes for 2, 3, 4, and 5 years are calculated (see Table A5 and Table A6 in the Appendix). These results are shown in Figure 13 and summarized in Table 4.

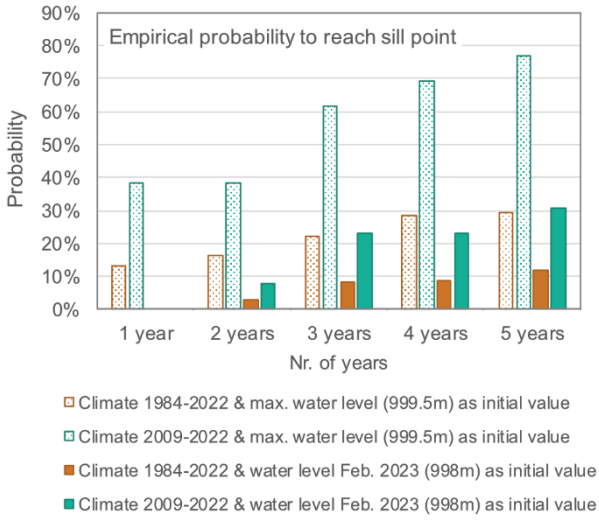

Figure 13: Empirical probability of lake levels to reach the sill point elevation based on observed year-to-year changes in water levels (Figure 12). The probability is evaluated for (i) two different climate assumptions (1984–2022 (long-term) and 2009-2022 (wet)) and (ii) two different water levels as initial value or starting point (maximum observed value of 999.5 m and water level of Feb. 2023 (998 m)). The probability includes the observed temporal sequences of lake level fluctuations, anticipating 1 to 5 years sequences.

Table 4: Empirical probabilities of lake level to reach sill point elevation based on observed year-to-year changes in lake water levels.

Assumption regarding		Empirical probability to reach sill point elevation in				
Initial lake level	**Climate conditions**	**1 year**	**2 years**	**3 years**	**4 years**	**5 years**
Maximum observed water level 1984–2020	Climate 2009-2022 (wet)	38%	38%	62%	69%	77%
	Climate 1984–2022 (long-term)	13%	16%	22%	29%	29%
Water level February 2023	Climate 2009-2022 (wet)	0%	8%	23%	23%	31%
	Climate 1984–2022 (long-term)	0%	3%	8%	9%	12%

The risk or empirical probability of lake levels to reach the sill point elevation depends on three factors regarding (i) climate conditions, (ii) the initial lake level and (iii) years anticipated for the lake to overflow. For the wetter climate assumption and the maximum observed lake level, the risk for the overflow lay between 38% to 77%, depending on the considered number of years. When assuming the long-term and overall drier climate, the risk for the overflow was lower, even for the maximum water level case. Here, again depending on the number of years considered, the risk lay between 13% and 29%.

The lake levels have fallen by 1.5 m and currently lie around 998 m. The risk of overflow has fallen accordingly. Assuming wetter climate conditions (long-term climate), the risk now lies between 0% and 31% (0% – 12%), depending on the anticipated number of years.

3.5 Rainfall conditions for a sustained flow

Specific rainfall and climate conditions in the Lake Bogoria watershed (1060 km²) lead to lake level fluctuations and to observed changes in lake level and lake volume. Based on the DAHITI lake volume variation data (Figure A3 and Table A3 in the Appendix), year-to-year changes can be calculated. These year-to-year changes in lake volume variation are then used to calculate the Integrated Catchment Response (ICR, mm) depicted in Figure 14 (Table A4). Note that volume variation data is only available until the end of 2020 and was not recalculated for this study, as was the case for the water levels.

The ICR is a magnitude that integrates all potential processes of the water balance of the lake and thus includes rainfall less evapotranspiration fluxes, year-to-year storage changes, but also potential sub-surface flows towards and from the lake. For example, in Figure 14, the high ICR of around 50 mm in 2019–2020 led to a lake level rise of 1.7 m as shown in Figure 12. In contrast, negative ICR-values lead to a decline in water level, e.g., between 2004–2005 or 2014–2015. This pattern is true for all years, except for 2015–2016, where the data shows a decline in water level of around 0.5 m, but a slight increase in ICR (see Figure A4 for a systematic comparison of ICR and water level).

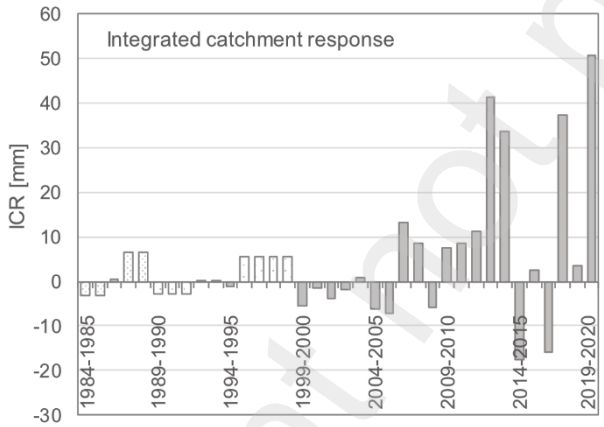

Figure 14: Integrated catchment response [mm] for 1984–2020 derived from year-to-year changes of lake volume variation. The dotted bars show years, where linear interpolation was necessary due to missing lake volume variation data.

Lake volume variation data is a function of data on water level and lake extent (Schwatke et al., 2020). The reason for the inconsistency between lake level and lake volume variation in these single years may lie in different data basis and inconsistencies therein. After 2016, lake levels are available from altimetry data, which is more trustworthy compared to the water levels before 2016, which are derived from hypsometry. Hypsometry defines a relationship between surface area and water level. It is used to extend water level data to periods where satellite altimetry was not available and is associated with higher uncertainties, also resulting from potential biases in estimates of lake area. For the current assessment we removed single water level and lake

variation data points from the time series, which were with high certainty biased, e.g. showing a very strong increase or decrease in a single time step, neglecting the overall trend. This however did not resolve the inconsistency between lake level and ICR for 2015–2016.

The difference between rainfall and ICR yields the actual catchment evapotranspiration AET (Eq. (4)), with which the ratio between actual evapotranspiration and rainfall can be calculated. The relationship between rainfall and the partitioning of actual evapotranspiration and rainfall for the Bogoria catchment is illustrated in Figure 15. This relationship is calculated for 2-, 3-, 5-, and 10-years moving averages, with the idea to smooth out effects of catchment storage from one year to the next in the water balance, but also potential errors in single year observations.

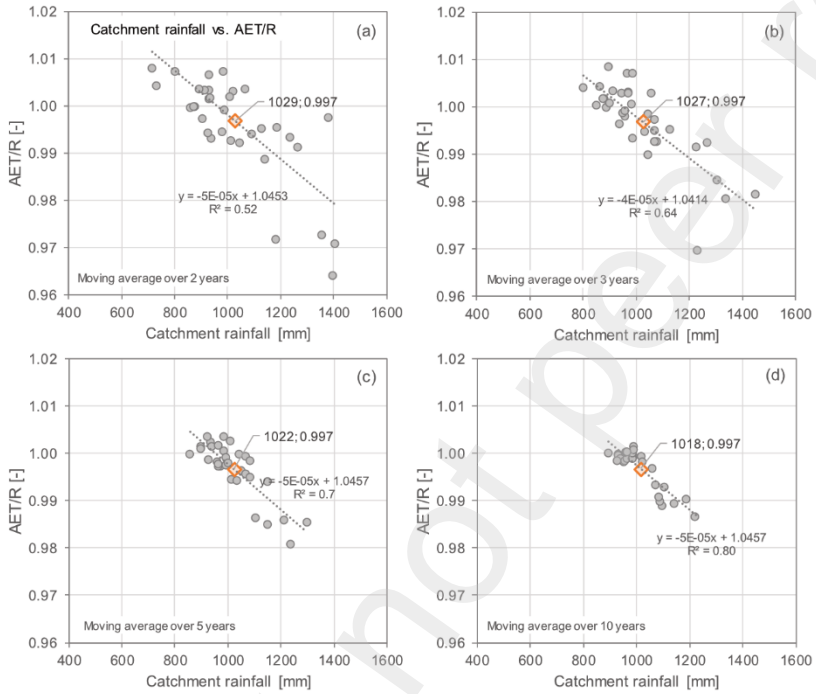

Figure 15: Relationship between rainfall and partitioning of actual evapotranspiration (AET) and catchment rainfall (R), calculated as 2-, 3-, 5- and 10-years moving averages and shown in panel (a)-(d). The labelled point corresponds to the average rainfall and AET/P-ratio for the period 1984–2020. All values refer to catchment averages.

Independent of the number of years used for calculating the moving average, the results show that a very high percentage – on average 99.7% – of catchment rainfall is lost to actual evapotranspiration. Thus, only around 0.3% of rainfall feeds the lake on average. The data of 2-year averages (Figure 15 (a)) shows that wetter years with higher rainfall show a slightly lower AET to R ratio, which lies around 97%. On the other hand, dryer conditions with lower rainfall lead to ratios above unity. In these years, catchment AET was higher compared to rainfall and the lake levels decreased. This pattern is also evident for the longer-term moving averages. Although the stronger year-to-year variability is somewhat lost, the main finding that only a very small fraction of the catchment rainfall feeds the lake, is still evident.

To derive the rainfall conditions necessary for a sustained flow from Lake Bogoria towards Lake Baringo, we derive a relationship or transfer function between the ICR and the CHIRPS-based catchment rainfall. This relationship is shown in Figure 16, again for different moving average windows. Positive ICR-values and corresponding rainfall refer to periods where lake levels increased. As with AET/R, smoothing of the data using longer-term moving averages leads to a loss of variability, but an increase in the coefficient of determination R^2.

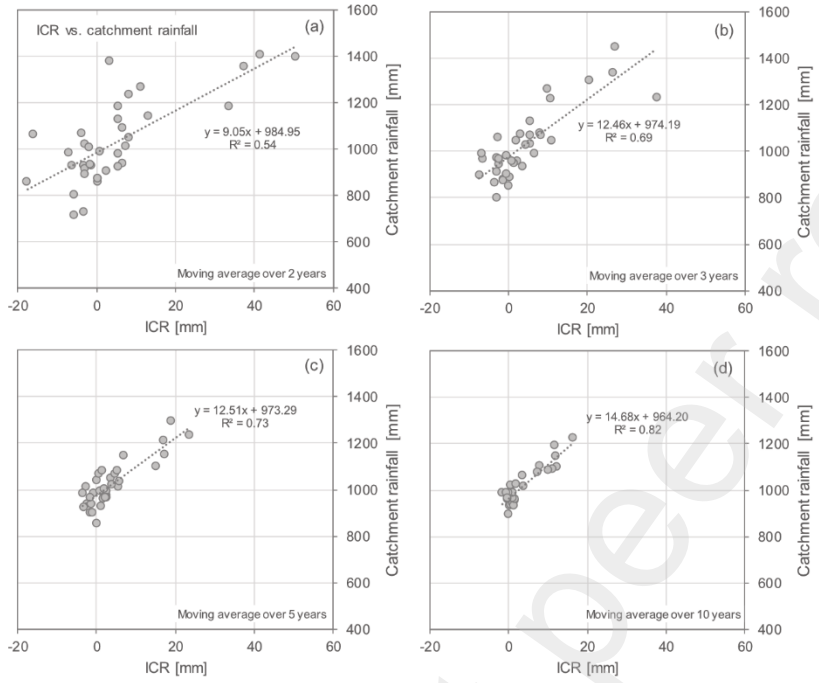

Figure 16: Relationship between Integrated Catchment Response (ICR) and catchment rainfall calculated as 2, 3, 5 and 10 year moving averages shown in panels (a)-(d). Data from 1984–2020 is shown.

Given the case that lake levels are at sill point elevation, additional discharge into the lake would lead to an overtopping and flow towards Lake Baringo. The quantity of flow would depend on the quantity of water feeding Lake Bogoria. This is the sum of different sources, including flows from the seasonal Waseges or Sandai River, the thermal springs or rainfall on the lake and are reflected in Figure 16.

For this analysis, we assume different sustained flow scenarios, which refer to mean annual discharge values. The flow would probably experience temporal variability. This we ignore here and estimate a mean annual flow.

The mean annual flow can be related to an annual volume, which would be needed to sustain a flow over one year. The mean flow values (in L/s or dm^3/s) are multiplied by the number of seconds in a year and then divided by the catchment area in [m^2]. This results in a mean runoff depth of the catchment to provide such a water volume that the condition of sustained flow is satisfied. Here, we provide several scenarios ranging from 10 L/s to 1500 L/s or 1.5 m^3/s (Table 5).

Table 5: Sustained flow scenarios [L/s], including translated volume per year and necessary runoff to enable the sustained flow. All flows refer to mean annual values.

Sustained flow scenario (annual average) [L/s]	Volume [m³/a]	Necessary runoff depth towards lake to enable sustained flow [mm/a]
10	315 360	0.3
25	788 400	0.7
50	1 576 800	1.5
100	3 153 600	3
150	4 730 400	4.5
500	15 768 000	14.9
1000	31 536 000	29.8
1500	47 304 000	44.6

The runoff depths for the different flow scenarios depend on rainfall and the partitioning of AET to rainfall (Figure 15). They are also related to the ICR and result from specific mean annual rainfall conditions (Figure 16). It is therefore possible to use the linear relationships shown in Figure 16 to derive, as a function of the necessary runoff depth, which corresponds to the ICR, the related catchment rainfall value. The rainfall conditions we estimate thereby refer to longer-term annual averages, since this is also the data basis for the relationships. Figure 17 shows the mean annual rainfall conditions which – given the case that Lake Bogoria water levels are at sill point elevation – would be necessary to provide a sustained flow of different magnitudes as shown on the x-axis. Mean annual flows of 500-1000 L/s would have been sustained with the mean annual rainfall value for 2010–2020. In contrast, it is also visible that on average no sustained flow would have been possible under rainfall conditions before 2010.

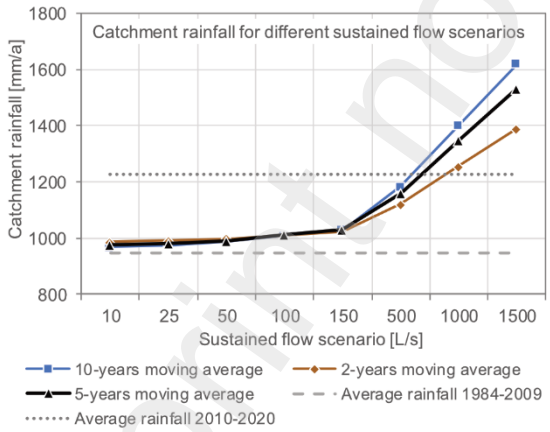

Figure 17: Simulated mean annual catchment rainfall for different sustained flow scenarios from Lake Bogoria towards Lake Baringo, given the case that lake levels are at sill point elevation. The estimate depends on the number of years used to estimate the transfer function. Average annual rainfall for 1984-2009 and 2010–2020 are plotted for reference and show that a mean annual flow of 500-1000 L/s would have been sustained with the mean annual rainfall value for 2010–2020.

Finally, Figure 18 shows the simulated rainfall values based on the 5-years moving average model and their corresponding sustained flow scenarios in relation to the observed catchment rainfall values in the past 37 years. It is visible that after 2010, mean annual rainfall of around

1230 mm/a was high enough to – on average – provide a flow of 500-1000 L/s. In the period 1984–2009 with a mean rainfall of around 950 mm/a, on average no flow would have been sustained.

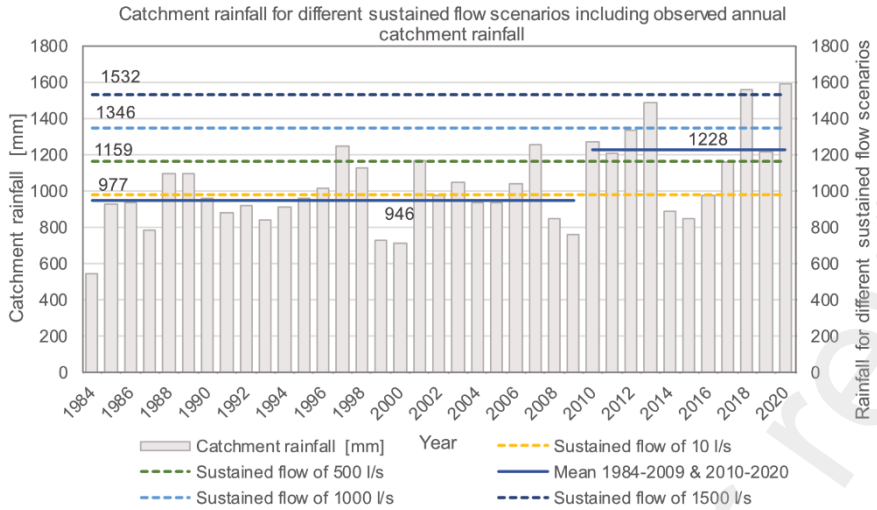

Figure 18: Observed annual catchment rainfall for Bogoria, including averages (1984–2020 and different average rainfall values for sustained flow scenarios ranging from 10 L/s to 1500 L/s.

4 Discussion

4.1 Sill point and risk of overflow

Only additional 70 cm lake level increase would have been necessary that Lake Bogoria reaches the sill point elevation of 1000.2 m, compared to the maximum observed lake levels in November 2020 of 999.5 m. The likelihood or empirical chance of Lake Bogoria's water levels reaching the sill point elevation is dependent on the assumptions made about (i) climate conditions, (ii) the initial lake level, and (iii) the number of years anticipated for the lake to overflow significantly influence the risk assessment.

For scenarios assuming wetter climate conditions as we have observed in the last decade and the maximum observed lake level, the risk of overflow was found to range between 38% and 77%, depending on the projected time frame. However, when considering long-term climate conditions, the risk of overflow decreased, even for the case of the maximum water level, varying between 13% and 29%. Presently, the lake levels have declined by 1.5 meters, and the current level is approximately 998 m. Consequently, the risk of overflow has decreased accordingly. With assumptions of wetter climate conditions (or the long-term climate), the risk now lies between 0% and 31% (or 0% to 12%), depending on the projected time frame.

The research suggests that the risk of Lake Bogoria reaching the sill point is generally higher when using the wetter period 2009–2022 as a reference for climate conditions. This period exhibited increased precipitation and resulted in significantly higher lake level fluctuations

compared to historical data. Additionally, the risk is amplified when considering not only one year but multiple years (up to 5 years) of observed lake level fluctuations for the empirical risk calculation.

The initial lake level assumption plays a crucial role in determining the risk. A lower initial lake level, such as the 998 m recorded in February 2023 (2.2 m below the sill point), leads to a reduced risk since the water levels would need to increase more substantially to reach the overflow point. Conversely, a higher initial water level assumption, like the maximum observed water level of 999.5 m (where the sill point was only 70 cm away), results in a higher risk of overflow.

In using the empirical probability to evaluate the risk of overtopping we assume that future climatic conditions are comparable to the past. We also assume that the temporal sequence of lake level fluctuations (and rainfall variability) between single years, so not only increases but also decreases, reflect the natural conditions of the system. In using the observed lake levels for the evaluation of the risk, changes in rainfall and the catchment water balance in general are intrinsically considered. The relationship between lake level and lake volume change are also inherently captured, since the lake level-volume-relationship is already considered in the year-to-year changes in the lake levels used as data basis. In these changes, the potential non-linearity between lake level and volume change, which is relevant regarding the quantity of inflows, on-lake rainfall and evaporation, is considered.

4.2 Trends in rainfall

Our research reveals significant and, in this detail, not observed meteorological and hydrological transformations occurring in the Rift Valley lakes of Kenya. By examining data collected from the Marigat station, located approximately 30 km northwest of Lake Bogoria, we have found remarkable shifts in the temporal patterns. Over the past decade, the average annual rainfall has more than doubled, accompanied by a substantial increase in rainfall variability. Notably, the number of days experiencing intense rainfall has increased by nearly 320% . These extraordinary changes, which have not been previously examined, particularly in relation to the ongoing elevation of lake levels, underscore the unique nature of this hydrometeorological phenomenon in the Rift Valley.

The rainfall increase suggested by the Marigat data is exceptional. There are numerous cases in eastern Africa of individual years reaching the extremely anomalously values. However, a step function increase in sustained rainfall of the magnitude seen at Marigat is very unusual. Nevertheless, several observations suggest that the trends at Marigat are realistic.

It is relevant that the greatest variability in monthly totals is for the three months of the boreal summer, July through September, which is the driest season of most of eastern Africa. The increase is particularly strong in July. Ideally one would make a comparison with nearby stations, but the available data are limited. However, at nearby Nakuru average July rainfall for the period 2010 to 2013 was 142 mm, one standard deviation above the long-term July mean of 96 mm. As in the Marigat record, the wettest July was 2013. Rainfall was 174 mm in that year, nearly two standard deviations above the mean of 96 mm. The excellent agreement between year-to-year changes in the level of Lake Bogoria and rainfall at Marigat helps to confirm the Marigat record (Nicholson and Yin, 2001). The trends in the levels of Lake Bogoria are also matched by those at lakes Baringo, Elementaita, Nakuru, Naivasha, and Solai (Herrnegger et al., 2021).

The changes seen in the area of these lakes are not representative of East Africa as a whole. There, annual rainfall has been stable in recent years, while October-November rainfall has increased and March-April-May rainfall has decreased (Nicholson et al., 2018). However, the tremendous increase in the level of Lake Bogoria of 2019/20 does correspond to a major wet episode throughout the region (Nicholson et al., 2022).

The meteorological factors affecting Lake Bogoria are complex. An important one is that it lies at the transition to boreal summer rainfall to the west. In fact, its variations are more closely link to that region that to those elsewhere in eastern Africa (Nicholson, 2019). A case in point is the similar trends in western Uganda, as seen at the station Arua. There the mean for 2010 to 2016 was 214 mm, considerably greater than the long-term mean of 149 mm. A small eastward shift in the boreal summer rainfall regime can account for the large July-to-September increases seen at Lake Bogoria. A second factor is that Lake Bogoria and the other lakes mentioned lie upon a ridge of the Rift Valley. Orographic factors can markedly enhance variations in rainfall.

The local-scale changes are notably more pronounced when compared to the average changes observed in the entire catchment area. In the study conducted by Herrnegger et al. (2021), it was demonstrated that the average rainfall within the Lake Bogoria catchment increased by approximately 30% during the period of 2010–2020, compared to the period of 1984-2009. This increase in rainfall has consequently led to rises in lake levels but also expansion of vegetation.

4.3 Vegetation increases

As illustrated in Figure 2 of the current work, there has been a noticeable expansion in vegetation cover as measured by the NDVI, with many regions experiencing growth rates exceeding 10% between 2001–2009 and 2010–2020.

This transformation in vegetation serves as an additional indicator of heightened rainfall and challenges the assertions made by other experts that attribute the lake level increases to alternative causes. It has been speculated that the tectonic activities occurring in the geologically active Rift Valley have diminished underground seepage, which serves as the sole outflow for the endorheic lakes, thus contributing to the elevation of lake levels. Moreover, anthropogenic land degradation has been proposed as a factor, resulting in increased erosion and sedimentation rates, potentially obstructing and impeding the underground water pathways while augmenting surface runoff. Our findings firmly support the notion that changes in rainfall alone are sufficient to account for the observed rises in lake levels.

4.4 Use of catchment averages for the assessment

The assessment of the hydrometeorological conditions contributing to the elevation of lake levels, as well as the examination of sustained overflow, is conducted based on the average rainfall observed within the catchment area. The watershed or catchment of Lake Bogoria encompasses a larger region of approximately 1060 km², spanning a maximum width of 30 km from west to east and extending around 60 km to the south from the sill point.

It is important to consider that spatial and temporal variations in rainfall exist within this area, as demonstrated through our analysis of the Marigat station data. The headwater regions of the Waseges River receive an annual rainfall of approximately 1200-1500 mm, while the southern vicinity of Lake Bogoria and the western parts of the catchment experience notably drier conditions (refer to Figure 7 in Herrnegger et al. (2021)). Station data from the northern area of Lake Bogoria indicate an average annual rainfall of around 700 mm between 1976 and 2001 (Ashley et al., 2004).

To estimate the water balance of Lake Bogoria, we rely on catchment average rainfall and lake volume variations. This approach assumes that (i) catchment boundaries are correct and (ii) the properties of lake levels can be adequately modeled using the average rainfall across the catchment area, disregarding the spatial and temporal variability of rainfall. However, our results demonstrate that employing longer-term aggregated rainfall data establishes a strong relationship with changes in lake levels and volume. As a result, we have confidence in the

validity of this approach for assessing the water balance and fluctuations in water levels of the lake.

4.5 AET/R ratio

Our findings reveal that, in relation to the entire catchment of Lake Bogoria, only a small fraction of rainfall contributes to the lake. The ratio of actual evapotranspiration to rainfall (AET/R) indicates that, during wetter years, approximately 3% of rainfall reaches the lake, while on average, only 0.3% of rainfall directly replenishes the lake. More than 97% of the rainfall is lost to evapotranspiration. Average potential evapotranspiration lies around 2600 mm/a for the Lake Bogoria catchment (Herrnegger et al., 2021) and is thus around 2.5 times higher compared to annual rainfall, suggesting that there is sufficient energy potential for evapotranspiration. It is crucial to emphasize that these percentages are based on catchment averages and may overlook the possibility that the lake receives a more substantial contribution from local rainfall. This local variability is not considered in our analysis, and thus, the results should be interpreted as a representation of the catchment water balance. The partitioning of AET/R in the headwaters of the Waseges River will exhibit different dynamics. Also, the calculated AET/R ratio includes anthropogenic influences and water abstractions affecting the water balance, since e.g. the Waseges River is also used for irrigation and food production in the headwaters.

4.6 Uncertainties

The assessment is subject to various uncertainties stemming from both the input data utilized and the adoption of simplified methods and assumptions as highlighted before in the context of using catchment average rainfall values.

The assessment of the sill point location and elevation is based on different digital elevation models. They differ regarding spatial resolution but also methods used to derive the elevation values. Also, different vertical datums are present in the elevation data sets, so that corrections had to be applied. These transformations always include uncertainties. To assess the sill point elevation and to reduce the uncertainties, a geometric terrestrial survey would probably be the best option.

Our analysis of the water balance and hydrological changes in Lake Bogoria heavily relies on satellite-based data, primarily the CHIRPS rainfall data. While this data source offers the advantage of providing insights into the spatial distribution and variability of rainfall, it is important to acknowledge that uncertainties exist regarding the accuracy of the quantities

recorded, despite efforts to enhance it with station data. It can at the same time be noted that the CHIRPS data generally shows good performance in the study region (Omonge et al., 2022). Additionally, the DAHITI data also introduces uncertainties into our analysis. Specifically, the water extent data exhibits partial biases and necessitates critical review. Consequently, the water level data derived from hypsometry, reliant on the water extent information, also carries uncertainties that need to be acknowledged.

For assessing the risk of Lake Bogoria to reach the sill point, we use the concept of empirical probability. It solely relies on the measured lake level data, which we assume describes the natural variability in a sufficient manner. The empirical probability does not make any assumptions regarding a specific statistical models or probability distribution. The application is transparent; no additional parameters need to be estimated. A disadvantage however may lie in the comparatively short time series used. Although 40 years of lake level data ranging from 1984 to 2023 are used, it is uncertain to what extent this time series covers the natural variability.

The estimation of the AET/R ratio, but also rainfall conditions necessary for a sustained flow, uses the ICR as input. In the application of the ICR we assume that underground seepage and outflows from Lake Bogoria are either (i) very small and thus negligible or (ii) stationary in time. Lying in an endorheic basin, Lake Bogoria does not have surface runoff. For the case that substantial underground losses to Lake Baringo do exist, the estimation of AET would be too high and the ratio between AET/R would be lower values, compared to our results. For the case that the outflows show substantial changes with time, the use of lake volume variation data and the ICR would probably not be appropriate since boundary conditions would change from year to year making it difficult to distinguish between changes in the hydrological regime of the catchment and underground outflow. However, based on the information available to us, there is no evidence to suggest substantial underground losses in Lake Bogoria. The lake's high alkalinity supports this hypothesis, as it indicates that no salts are being flushed out through underground pathways. Unlike Lake Baringo, where hot springs in Kapedo might serve as an outflow location for seepage waters, we don't have any apparent similar springs in Lake Bogoria, at least to our knowledge.

4.7 Potential impacts

Eight to ten thousand years ago lake levels were significantly higher. South of Lake Turkana the 300 m deep Lake Suguta with a surface area of around 2150 km² existed (Garcin et al., 2009) and the catchment boundaries were very different (Dommain et al., 2022). Lake Bogoria

and Baringo were connected and drained to the north towards this ancient lake. If Lake Bogoria were to overflow, several effects would ensue, both in the short and long term.

In the short term, there would be a potential cross-contamination of the alkaline waters from Bogoria, impacting the now freshwater Kiborkoch, Loboi, and Ng'arua Swamps, as well as the watercourse of the potential stream. These also includes the lower stretch of the current Molo River and ultimately Lake Baringo itself. The specific nature of these cross-mixing and dilution effects is currently uncertain and requires further investigation. The Loboi plain experiences exceptionally high potential evapotranspiration rates, resulting in substantial water losses that may strongly reduce the water reaching Lake Baringo. Hence, additional research is necessary to assess and comprehend potential dilution effects.

On a longer time scale, assuming a sustained and significant overflow of Lake Bogoria coupled with above-average runoff reaching Lake Baringo, the lake levels of Lake Baringo would continue to rise. However, Lake Baringo would not rise until it reaches an equilibrium with the sill point elevation of Lake Bogoria. Prior to that, the sill point of Lake Baringo (Lobat Gap), which sits approximately 9.7 m lower than the sill point of Lake Bogoria at 990.5 m, would be exceeded, leading to the outflow of water towards the Suguta Basin in the north, a situation reminiscent of conditions approximately eight to ten thousand years ago (see contours of sill point elevations in Figure 4 and potential water extents in Figure A5). Nevertheless, it is crucial to acknowledge that such changes would be dramatic and significantly impact the lives and livelihoods of tens of thousands of people in the area.

4.8 Mitigation measures

The rise in lake levels is primarily influenced by changes in rainfall, and our ability to control these causes is limited. Our focus should be on mitigating the symptoms to some extent and preparing ourselves as a society to adapt to these changes. Water retention measures can be taken in the lake watersheds, with the aim to hold back water in the catchments (Stecher et al., 2023). Afforestation, implementation of soil water conservation measures, enforcing infiltration of rainfall and surface runoff by technical and natural means are beneficial (Mwanake et al., 2023; Nyirahabimana et al., 2021; Turinawe, 2019). They are no-regret measures and tend to increase infiltration to groundwater, but also reduce flood peaks. These measures can milden the situation, but also have other positive effects on the landscape and ecosystem services in general.

At Lake Bogoria, options also exist to implement technical measures. The topographic conditions in the area of the Lake Bogoria sill point would provide a good setting for

constructing a dam to artificially increase the sill point elevation. Careful investigations would however be essential before such measures are taken to understand the potential effects of such an undertaking, including an assessment of the effects on the local community but also environmental effects on flora and fauna and the ecosystem in general.

Given the low level of availability and accessibility of measured hydroclimatic data on the ground, it is challenging to evaluate and provide clearer understanding of the on-going phenomenon. The expansion of the measurement network of rainfall and discharge to an extent as had already existed (so nothing new) and the careful consideration of data quality in the observations would allow for a more solid basis for planning and understanding the lake level rises, including the potential overtopping of Lake Bogoria. Independent from that, the information and data would be essential for water resources planning, allocation and management in general (Omonge et al., 2020). For dynamic developing nations like Kenya, the sustainable planning of water resources is essential and should ground on a solid objective data basis, i.e. trustworthy and available measurements.

Preparedness is a category in flood risk management, which can significantly reduce human and economic losses. Anticipatory flood risk maps showing riparian areas, relevant or critical infrastructure such as roads, hospitals or schools, which may be flooded if lake levels continue to rise, would make the natural phenomenon more plannable and approachable. Including historic high stands of water levels would put into perspective, what may be a worst-case scenario. And this information must be understood and made available to people on the ground. Reports, maps and data on the desks of researchers and administrators will hardly help.

5 Summary and Conclusions

Starting around 2010, several Rift Valley lakes of Kenya have experienced significant rises in water levels. Nearly eighty thousand households with 400,000 people are affected. There is fear of an ecological catastrophe, should the current water levels of the alkaline Lake Bogoria continue to rise. The result would be an overflow and mixing with the freshwater Lake Baringo. This research therefore examines the risk of Lake Bogoria reaching its sill point, leading to an overflow towards Lake Baringo, a situation present around 8 000–10 000 years ago.

The data reveal significant meteorological and hydrological changes in the region over the past decade. For Marigat, located at the edge of the Loboi plain, average annual rainfall has more than doubled (+111%), accompanied by a substantial increase in rainfall variability with an average over all month of +200%. Although the number of days with rainfall has decreased in the last decade (-19%), the number of days experiencing intense rainfall has increased by

+318%. Overall, these changes have made planning based on the well-known rainfall seasons more difficult.

Regarding the sill point, results show that only an additional 70 cm increase in lake level would have been necessary for Lake Bogoria to reach the tipping point of 1000.2 m from its maximum observed level in November 2020, which was 999.5 m. The risk of overflow is influenced by climate conditions, and assuming wetter climate conditions observed in the last decade, the risk ranges from 38% to 77% depending on the number of years of lake level fluctuations anticipated in the assessment. However, with long-term climate conditions of 1984 to 2022, the risk decreases to 16% to 29%.

Currently, the lake level has declined by 1.5 m to approximately 998 m, resulting in a decreased risk of overflow. Under the assumptions of wetter climate conditions from the last decade (or long-term climate), the risk is now between 0% and 23% (or 0% to 9%).

The results regarding partitioning of actual evapotranspiration and rainfall indicate that on average around 99.7% of catchment rainfall is lost to AET, leaving only about 0.3% to feed the lake. Wetter years with higher rainfall show a slightly lower AET to rainfall ratio (around 97%), while drier years with lower rainfall have ratios above unity, resulting in decreased lake levels.

Assuming that the climate stays as wet as in the last decade, the risk of Lake Bogoria reaching the sill point lies at around 20% when assuming current lake levels. Given that water levels of Lake Bogoria are at sill point elevation, we provide several scenarios for a sustained flow towards Baringo. Here, results indicate that mean annual catchment rainfall of around 1230 mm/a observed after 2010 was high enough to provide an average annual flow of 500-1000 L/s, while during the period 1984–2009, with a mean rainfall of around 950 mm/a, no sustained flow would have been possible on average.

If Lake Bogoria were to overflow today, it would have both short-term and long-term effects. In the short term, there could be potential cross-contamination of the alkaline waters from Lake Bogoria, impacting the watercourse of the potential stream and freshwater ecosystems like Kiborkoch, Loboi, and Ng'arua Swamps, and finally Lake Baringo. The Loboi plain experiences high evapotranspiration rates, leading to significant water losses that could however reduce the water reaching Lake Baringo. The specific effects of this mixing and dilution are not yet understood and require further investigation. On a longer time scale, assuming a sustained and significant overflow of Lake Bogoria with above-average runoff reaching Lake Baringo, the lake levels of Lake Baringo would continue to rise. However, before reaching equilibrium with the sill point elevation of Lake Bogoria, Lake Baringo's water levels

would rise past its sill point elevation at the Lobat Gap, which is about 9.7 meters lower than that of Lake Bogoria (at 990.5 meters). This would lead to the outflow of water towards the Suguta Basin in the north, a situation reminiscent of conditions thousands of years ago. Such changes would be drastic and have a significant impact on the lives and livelihoods of thousands of people in the area.

The rise in lake levels is mainly driven by changes in rainfall, and while we have limited control over these causes, we can focus on mitigating the symptoms and preparing society for adaptation. At Lake Bogoria, technical measures like constructing a dam to artificially increase the sill point elevation are possible, but careful investigations are necessary to understand potential effects on the community and environment.

The lack of sufficient hydroclimatic data makes it challenging to fully understand the ongoing phenomenon. Expanding the measurement network for rainfall and discharge would provide a more solid basis for planning and understanding the lake level rises. This data is essential for water resources planning, allocation, and management in Kenya. Preparedness, including flood risk maps and information about historic high-water levels, can significantly reduce human and economic losses, but it's crucial to ensure that this information is accessible and understood by people on the ground, not just confined to researchers and administrators.

In conclusion, the research shows that Lake Bogoria's risk of reaching the sill point and overflowing is not negligible and is dependent on various factors, particularly climate conditions and the initial lake level. The findings suggest that managing water resources and preparing for potential overflow scenarios are crucial, especially with the observed meteorological and hydrological transformations in the region.

6 Author contributions

MH, GS and PK designed the study and established the methodological framework. MH, GS, NC, LO and DO participated in the field work for the study. MH, PK and GS performed all analyses. MH prepared the maps and figures. MH drafted and compiled the manuscript with contributions, checks and revisions by all other co-authors.

7 Data availability

The study was mostly performed using openly available primary input data. All these input data can be acquired from the rights holders of these data sets. All intermediate and final data that were generated in this study are available upon request to the corresponding author, assuming concrete requests.

8 Competing interests

The authors declare that they have no conflict of interest.

9 Acknowledgments

Assistance in understanding issues regarding differences in vertical datums of the elevation data and geoid undulations was provided by Reinfried Mansberger. Peter Odwe and Fredrick A. Onyango performed the UAS flights. Sospeter Wekesa assisted in data collection. All this is highly acknowledged.

10 Financial support

This study is performed within the project "Water Level Fluctuations and Implications on Local Livelihoods in the Great Rift Valley Lakes of Kenya | GreatLakes" (KOEF 08/2020), financed by the Austrian Federal Ministry of Education, Science and Research within the programme „Cooperation Development Research" and administered by OeAD-GmbH / Austria's Agency for Education and Internationalisation.

High-resolution TanDEM-X terrain data is provided by the German Aerospace Center (DLR) and was awarded with the proposal ID DEM_HYDR3478.

11 References

Agembe, S., Ojwang, W., Olilo, C., Omondi, R., Ongore, C., 2016. Soda Lakes of the Rift Valley (Kenya), in: The Wetland Book. Springer Netherlands, Dordrecht, pp. 1–11. https://doi.org/10.1007/978-94-007-6173-5_150-1

AgiSoft, 2016. AgiSoft.

Ashley, G.M., Maitima Mworia, J., Muasya, A.M., Owen, R.B., Driese, S.G., Hover, V.C., Renaut, R.W., Goman, M.F., Mathai, S., Blatt, S.H., 2004. Sedimentation and recent history of a freshwater wetland in a semi-arid environment: Loboi Swamp, Kenya, East Africa. Sedimentology 51, 1301–1321. https://doi.org/10.1111/j.1365-3091.2004.00671.x

Avery, S., 2020. Kenya's Rift Valley lakes have been this high before. But there's cause for concern. The Conversation 1–4.

Avery, S.T., Tebbs, E.J., 2018. Lake Turkana, major Omo River developments, associated hydrological cycle change and consequent lake physical and ecological change. J Great Lakes Res 44, 1164–1182. https://doi.org/10.1016/j.jglr.2018.08.014

Becht, R., Mwango, F., Muno, F., 2006. Groundwater links between Kenyan Rift Valley lakes, in: Odada, E.O., Olago, D.O., Ochola, W., Ntiba, M., Wandiga, S., Gichuki, N., Oyieke, H. (Eds.), Journal of Chemical Information and Modeling. p. 12.

Bessems, I., Verschuren, D., Russell, J.M., Hus, J., Mees, F., Cumming, B.F., 2008. Palaeolimnological evidence for widespread late 18th century drought across equatorial East Africa. Palaeogeogr Palaeoclimatol Palaeoecol 259, 107–120. https://doi.org/10.1016/j.palaeo.2007.10.002

Busetto, L., Ranghetti, L., 2016. MODIStsp: an R package for preprocessing of MODIS Land Products time series. Comput Geosci 97, 40–48. https://doi.org/10.1016/j.cageo.2016.08.020

Darling, W.G., Allen, D.J., Armannsson, H., 1990. Indirect detection of subsurface outflow from a rift valley lake. J Hydrol (Amst) 113, 297–306. https://doi.org/10.1016/0022-1694(90)90180-6

Darling, W.G., Gizaw, B., Arusei, M.K., 1996. Lake-groundwater relationships and fluid-rock interaction in the East African Rift Valley: Isotopic evidence. Journal of African Earth Sciences 22, 423–431. https://doi.org/10.1016/0899-5362(96)00026-7

De Bock, T., Kervyn De Meerendré, B., Hess, T., Gouder De Beauregard, A.C., 2009. Ecohydrology of a seasonal wetland in the Rift Valley: Ecological characterization of Lake Solai. Afr J Ecol 47, 289–298. https://doi.org/10.1111/j.1365-2028.2008.00949.x

de Cort, G., Verschuren, D., Ryken, E., Wolff, C., Renaut, R.W., Creutz, M., van der Meeren, T., Haug, G., Olago, D.O., Mees, F., 2018. Multi-basin depositional framework for moisture-balance reconstruction during the last 1300 years at Lake Bogoria, central Kenya Rift Valley. Sedimentology 65, 1667–1696. https://doi.org/10.1111/sed.12442

Derakhshan, S., 2017. Ground and Surface Water Flow Modeling in the Lake Naivasha Basin. University of Twente.

Didan, K., 2015. MOD13Q1 MODIS/Terra Vegetation Indices 16-Day L3 Global 250m SIN Grid V006 [Data set]. NASA EOSDIS Land Processes DAAC. https://doi.org/10.5067/MODIS/MOD13Q1.006

Dommain, R.E., Riedl, S., Olaka, L.A., Demenocal, P., Deino, A.L., Bernhart Owen, R., Muiruri, V., M€, J., Potts, R., Strecker A Edited, M.R., Rinaldo, A., 2022. Holocene bidirectional river system along the Kenya Rift and its influence on East African faunal exchange and diversity gradients. https://doi.org/10.1073/pnas

Facebook Connectivity Lab and Center for International Earth Science Information Network - CIESIN - Columbia University, 2016. High Resolution Settlement Layer (HRSL). Source imagery for HRSL 2016 DigitalGlobe [WWW Document]. URL https://data.humdata.org/dataset/highresolutionpopulationdensitymaps-ken (accessed 9.21.23).

Flohn, H., 1987. East African Rains of 1961/62 and the Abrupt Change of the White Nile Discharge, in: Coetzee, J.A. (Ed.), Palaeoecology of Africa.

Funk, C., Peterson, P., Landsfeld, M., Pedreros, D., Verdin, J., Shukla, S., Husak, G., Rowland, J., Harrison, L., Hoell, A., Michaelsen, J., 2015. The climate hazards infrared precipitation with stations - A new environmental record for monitoring extremes. Sci Data 2, 1–21. https://doi.org/10.1038/sdata.2015.66

Garcin, Y., Junginger, A., Melnick, D., Olago, D.O., Strecker, M.R., Trauth, M.H., 2009. Late Pleistocene–Holocene rise and collapse of Lake Suguta, northern Kenya Rift. Quat Sci Rev 28, 911–925. https://doi.org/10.1016/j.quascirev.2008.12.006

Government of Kenya, UNDP, 2021. Rising Water Levels in Kenya's Rift Valley Lakes, Turkwel Gorge Dam and Lake Victoria - A Scoping Report.

Gregory, J.W., 1896. The Great Rift Valley : being the narrative of a journey to Mount Kenya and Lake Baringo : with some account of the geology, natural history, anthropology and future prospects of British East Africa / J.W. Gregory., The Great Rift Valley : being the narrative of a journey to Mount Kenya and Lake Baringo : with some account of the geology, natural history, anthropology and future prospects of British East Africa / J.W. Gregory. J. Murray, London : https://doi.org/10.5962/bhl.title.12499

Hassan, A.A., Jin, S., 2014. Lake level change and total water discharge in East Africa Rift Valley from satellite-based observations. Glob Planet Change 117, 79–90. https://doi.org/10.1016/J.GLOPLACHA.2014.03.005

Hassan, D., Burian, S.J., Johnson, R.C., Shin, S., Barber, M.E., 2023. The Great Salt Lake Water Level is Becoming Less Resilient to Climate Change. Water Resources Management 37, 2697–2720. https://doi.org/10.1007/s11269-022-03376-x

Herrnegger, M., Stecher, G., Schwatke, C., Olang, L., 2021. Hydroclimatic analysis of rising water levels in the Great rift Valley Lakes of Kenya. J Hydrol Reg Stud 36, 100857. https://doi.org/10.1016/j.ejrh.2021.100857

Ho, Y.F., Hengl, T., Parente, L., 2023. Ensemble Digital Terrain Model (EDTM) of the world (Version 1.1) [Data set]. https://doi.org/https://zenodo.org/record/7634679

Jarvis, A., Guevara, E., Reuter, H.I., Nelson, A.D., 2008. Hole-filled SRTM for the globe : version 4 : data grid. CGIAR Consortium for Spatial Information.

Jenny, J.P., Anneville, O., Arnaud, F., Baulaz, Y., Bouffard, D., Domaizon, I., Bocaniov, S.A., Chèvre, N., Dittrich, M., Dorioz, J.M., Dunlop, E.S., Dur, G., Guillard, J., Guinaldo, T., Jacquet, S., Jamoneau, A., Jawed, Z., Jeppesen, E., Krantzberg, G., Lenters, J., Leoni, B., Meybeck, M., Nava, V., Nõges, T., Nõges, P., Patelli, M., Pebbles, V., Perga, M.E., Rasconi, S., Ruetz, C.R., Rudstam, L., Salmaso, N., Sapna, S., Straile, D., Tammeorg, O., Twiss, M.R., Uzarski, D.G., Ventelä, A.M., Vincent, W.F., Wilhelm, S.W., Wängberg, S.Å., Weyhenmeyer, G.A., 2020. Scientists' Warning to Humanity: Rapid degradation of the world's large lakes. J Great Lakes Res 46, 686–702. https://doi.org/10.1016/J.JGLR.2020.05.006

Kast, J.B., Apostel, A.M., Kalcic, M.M., Muenich, R.L., Dagnew, A., Long, C.M., Evenson, G., Martin, J.F., 2021. Source contribution to phosphorus loads from the Maumee River watershed to Lake Erie. J Environ Manage 279, 111803. https://doi.org/10.1016/j.jenvman.2020.111803

Kiage, L.M., Douglas, P., 2020. Linkages between land cover change, lake shrinkage, and sublacustrine influence determined from remote sensing of select Rift Valley Lakes in Kenya. Science of the Total Environment 709, 136022. https://doi.org/10.1016/j.scitotenv.2019.136022

Kimaru, A.N., Gathenya, J.M., Cheruiyot, C.K., 2019. The Temporal Variability of Rainfall and Streamflow into Lake Nakuru, Kenya, Assessed Using SWAT and Hydrometeorological Indices. Hydrology 6, 88. https://doi.org/10.3390/hydrology6040088

Kray, P., 2023. Analysis of the potential overflow of Lake Bogoria towards Lake Baringo, Kenya (Master / Diploma Thesis). Institute of Hydrology and Water Management, University of Natural Resources and Life Sciences, Vienna.

Lindsay, J.B., 2023. WhiteboxTools v2.3.

Liu, W., Zhou, G., Liu, H., Li, Qing-peng, Xie, C., Li, Qing, Zhao, J., Zhang, Q., 2023. Large-scale characteristics of thermokarst lakes across the source area of the Yellow River on

the Qinghai-Tibetan Plateau. J Mt Sci 20, 1589–1604. https://doi.org/10.1007/s11629-022-7693-y

McCall, J., 2010. Lake Bogoria, Kenya: Hot and warm springs, geysers and Holocene stromatolites. Earth Sci Rev 103, 71–79. https://doi.org/10.1016/j.earscirev.2010.08.001

Muita, R., Gikungu, D., Aura, S., Njogu, A., Ndichu, R., Nyinguro, P., Kiptum, C., 2021. Assessment of Rising Water Levels of Rift Valley Lakes in Kenya: The Role of Meteorological Factors. Environmental Sciences and Ecology: Current Research (ESECR) 2.

Mwanake, H., Mehdi-Schulz, B., Schulz, K., Kitaka, N., Olang, L.O., Lederer, J., Herrnegger, M., 2023. Agricultural Practices and Soil and Water Conservation in the Transboundary Region of Kenya and Uganda: Farmers' Perspectives of Current Soil Erosion. Agriculture 13, 1434. https://doi.org/10.3390/agriculture13071434

Nicholson, S., 2001. Climatic and environmental change in Africa during the last two centuries. Clim Res 17, 123–144. https://doi.org/10.3354/cr017123

Nicholson, S.E., 2019. A Review of Climate Dynamics and Climate Variability in Eastern Africa, in: The Limnology, Climatology and Paleoclimatology of the East African Lakes. Routledge, pp. 25–56. https://doi.org/10.1201/9780203748978-2

Nicholson, S.E., 1998. Historical Fluctuations of Lake Victoria and Other Lakes in the Northern Rift Valley of East Africa. pp. 7–35. https://doi.org/10.1007/978-94-017-1437-2_2

Nicholson, S.E., Fink, A.H., Funk, C., Klotter, D.A., Satheesh, A.R., 2022. Meteorological causes of the catastrophic rains of October/November 2019 in equatorial Africa. Glob Planet Change 208, 103687. https://doi.org/10.1016/j.gloplacha.2021.103687

Nicholson, S.E., Funk, C., Fink, A.H., 2018. Rainfall over the African continent from the 19th through the 21st century. Glob Planet Change 165, 114–127. https://doi.org/10.1016/j.gloplacha.2017.12.014

Nicholson, S.E., Yin, X., 2001. Rainfall conditions in equatorial East Africa during the nineteenth century as inferred from the record of Lake Victoria. Clim Change 48, 387–398. https://doi.org/https://doi.org/10.1023/A:1010736008362

Nyirahabimana, H., Turinawe, A., Lederer, J., Karungi, J., Herrnegger, M., 2021. What influences farmer's adoption lag for soil and water conservation practices? Evidence from

sio-malaba malakisi river basin of kenya and uganda borders. Agronomy 11, 1985. https://doi.org/10.3390/agronomy11101985

Obando, J.A., Onywere, S., Shisanya, C., Ndubi, A., Masiga, D., Irura, Z., Mariita, N., Maragia, H., 2016. Impact of Short-Term Flooding on Livelihoods in the Kenya Rift Valley Lakes, in: Geomorphology and Society. Springer, pp. 193–215. https://doi.org/10.1007/978-4-431-56000-5_12

Odada, E.O., Onyando, J., Obudho, P.A., 2006. Lake Baringo: Experience and Lessons Learned Brief, World Lake Basin Management Initiative: experience and lessons learned briefs.

Ojwang, W.O., Obiero, K.O., Donde, O.O., Gownaris, N., Pikitch, E.K., Omondi, R., Agembe, S., Malala, J., Avery, S.T., 2016. Lake Turkana: World's Largest Permanent Desert Lake (Kenya), in: The Wetland Book. Springer Netherlands, pp. 1–20. https://doi.org/10.1007/978-94-007-6173-5_254-1

Okech, E., Kitaka, N., Omondi, S., Verschuren, D., 2019. Water level fluctuations in Lake Baringo, Kenya, during the 19th and 20th centuries: Evidence from lake sediments. Afr J Aquat Sci 44, 25–33. https://doi.org/10.2989/16085914.2019.1583087

Olaka, L.A., Odada, E.O., Trauth, M.H., Olago, D.O., 2010. The sensitivity of East African rift lakes to climate fluctuations. J Paleolimnol 44, 629–644. https://doi.org/10.1007/s10933-010-9442-4

Omonge, P., Feigl, M., Olang, L., Schulz, K., Herrnegger, M., 2022. Evaluation of satellite precipitation products for water allocation studies in the Sio-Malaba-Malakisi river basin of East Africa. J Hydrol Reg Stud 39, 100983. https://doi.org/10.1016/j.ejrh.2021.100983

Omonge, P., Herrnegger, M., Gathuru, G., Fürst, J., Olang, L., 2020. Impact of development and management options on water resources of the upper Mara River Basin of Kenya. Water and Environment Journal 34, 644–655. https://doi.org/10.1111/wej.12554

Onywere, S., Shisanya, C., Obando, J., Ndubi, A., Masiga, D., Irura, Z., Mariita, N., Maragia, H., 2013. Geospatial extent of 2011-2013 flooding from the Eastern African Rift Valley Lakes in Kenya and its implication on the ecosystems, in: Papers, Kenya Soda Lakes Workshop. Kenya Wildlife Service Training Institute, Naivasha. p. 22.

OpenStreetMap contributors, 2023. OpenStreetMap data.

Owen, R.B., Renaut, R.W., 1986. Sedimentology, stratigraphy and palaeoenvironments of the Holocene Galana Boi Formation, NE Lake Turkana, Kenya. Geological Society, London, Special Publications 25, 311–322. https://doi.org/10.1144/GSL.SP.1986.025.01.25

Pavitt, N., 2008. Kenya: A Country in the Making, 1880-1940. W. W. Norton & Company.

Pekel, J.F., Cottam, A., Gorelick, N., Belward, A.S., 2016. High-resolution mapping of global surface water and its long-term changes. Nature 540, 418–422. https://doi.org/10.1038/nature20584

Petek, N., 2018. Archaeological perspectives on risk and community resilience in the Baringo Lowlands, Kenya, in: Studies in Global Archaeology. Department of Archaeology and Ancient History, Uppsala University, Uppsala, pp. 1–294.

Petek-Sargeant, N., 2023. Personal communication.

QGIS Development Team, 2023. QGIS Geographic Information System, Open Source Geospatial Foundation Project.

R Core Team, 2023. R: A Language and Environment for Statistical Computing.

Ramsar Convention, 2022. The List of Wetlands of International Importance.

Renaut, R.W., Owen, R.B., Ego, J.K., 2017. Geothermal activity and hydrothermal mineral deposits at southern Lake Bogoria, Kenya Rift Valley: Impact of lake level changes. Journal of African Earth Sciences 129, 623–646. https://doi.org/10.1016/j.jafrearsci.2017.01.012

Rexer, M., Hirt, C., 2016. Evaluation of intermediate TanDEM-X digital elevation data products over Tasmania using other digital elevation models and accurate heights from the Australian National Gravity Database. Australian Journal of Earth Sciences 63, 599–609. https://doi.org/10.1080/08120099.2016.1238440

Richardson, J.L., 1966. Changes in Level of Lake Naivasha, Kenya, during Postglacial Times. Nature 209, 290–291. https://doi.org/10.1038/209290a0

Robakiewicz, E., Owen, R.B., Rosca, C., Deino, A., Garcin, Y., Trauth, M.H., Kübler, S., Junginger, A., 2023. Hydroclimate reconstructions in the Suguta Valley, northern Kenya, during the Early-Middle Pleistocene Transition. Palaeogeogr Palaeoclimatol Palaeoecol 628, 111758. https://doi.org/10.1016/j.palaeo.2023.111758

Schwatke, C., Dettmering, D., Bosch, W., Seitz, F., 2015. DAHITI - An innovative approach for estimating water level time series over inland waters using multi-mission satellite

altimetry. Hydrol Earth Syst Sci 19, 4345–4364. https://doi.org/10.5194/hess-19-4345-2015

Schwatke, C., Dettmering, D., Seitz, F., 2020. Volume variations of small inland water bodies from a combination of satellite altimetry and optical imagery. Remote Sens (Basel) 12. https://doi.org/10.3390/rs12101606

Schwatke, C., Scherer, D., Dettmering, D., 2019. Automated extraction of consistent time-variable water surfaces of lakes and reservoirs based on Landsat and Sentinel-2. Remote Sens (Basel) 11. https://doi.org/10.3390/rs11091010

Shams Ghahfarokhi, M., Moradian, S., 2023. Investigating the causes of Lake Urmia shrinkage: climate change or anthropogenic factors? J Arid Land 15, 424–438. https://doi.org/10.1007/s40333-023-0054-z

Spears, B.M., Hamilton, D.P., Pan, Y., Zhaosheng, C., May, L., 2022. Lake management: is prevention better than cure? Inland Waters 12, 173–186. https://doi.org/10.1080/20442041.2021.1895646

Stager, J.C., Ryves, D., Cumming, B.F., Meeker, L.D., Beer, J., 2005. Solar variability and the levels of Lake Victoria, East Africa, during the last millenium. J Paleolimnol 33, 243–251. https://doi.org/10.1007/s10933-004-4227-2

Stecher, G., Hohensinner, S., Herrnegger, M., 2023. Changes in the water retention of mountainous landscapes since the 1820s in the Austrian Alps. Front Environ Sci 11. https://doi.org/10.3389/fenvs.2023.1219030

Strelnikova, D., Ioneanu, S., Herban, S., Paulus, G., Manfreda, S., 2022. Operations Manual for the Use of UAS in Environmental Studies (based on SORA 2.0). https://doi.org/10.5281/zenodo.7562377

Suess, E., 1891. Die Brüche des östlichen Afrika (The Rifts of East Africa), in: von Höhnel, L., Rosiwal, A., Toula, F., Suess, E. (Eds.), Beiträge Zur Geologischen Kenntniss Des Östlichen Afrika (Contributions to the Geological Knowledge of Eastern Africa). Denkschriften der Akademie der Wissenshaften. Mathematisch-Naturwissenschaftlichen Klasse.

Sutcliffe, J.V., Parks, Y.P., 1999. The Hydrology of the Nile. IAHS Special Publication 5, 192.

The EastAfrican, 2014. Tale of two lakes: Are Baringo and Bogoria likely to merge? [WWW Document]. URL https://www.theeastafrican.co.ke/tea/magazine/tale-of-two-lakes-are-baringo-and-bogoria-likely-to-merge--1334364 (accessed 2.16.23).

Tiecke, T.G., Liu, X., Zhang, A., Gros, A., Li, N., Yetman, G., Kilic, T., Murray, S., Blankespoor, B., Prydz, E.B., Dang, H.-A.H., 2017. Mapping the world population one building at a time.

Tiercelin, J.J., et al., 1987. Le demi-graben de Baringo-Bogoria, Rift Gregory, Kenya: 30.000 ans d'histoire hydrologique et sédimentaire, Bull. Centr. Rech. Expl.-Prod. Elf-Aquitaine.

Tower, A., Plano, R., 2023. "Climate change is controlling everything, let them compensate us" - Stories of loss & damage in Kenya.

Trauth, M.H., Strecker, M.R., 2019. Late Pleistocene Lake-Level Fluctuations in the Naivasha Basin, Kenya, in: The Limnology, Climatology and Paleoclimatology of the East African Lakes. Routledge, pp. 549–557. https://doi.org/10.1201/9780203748978-31

Turinawe, A., 2019. Impact of soil and water conservation technology adoption on smallholder farms in South-Western Uganda. J Dev Agric Econ 11, 217–233. https://doi.org/10.5897/jdae2018.0918

UNAVCO, 2021. Geoid Height Calculator [WWW Document]. URL https://www.unavco.org/software/geodetic-utilities/geoid-height-calculator/geoid-height-calculator.html (accessed 2.16.23).

UNESCO World Heritage Convention, 2023. World Heritage List [WWW Document]. URL https://whc.unesco.org/en/list/ (accessed 2.6.23).

Verschuren, D., 2019. Comparative Paleolimnology in a System of Four Shallow Tropical Lake Basins, in: The Limnology, Climatology and Paleoclimatology of the East African Lakes. Routledge, pp. 559–572. https://doi.org/10.1201/9780203748978-32

Verschuren, D., 2001. Reconstructing fluctuations of a shallow East African lake during the past 1800 yrs from sediment stratigraphy in a submerged crater basin. J Paleolimnol 25, 297–311. https://doi.org/10.1023/A:1011150300252

Verschuren, D., Laird, K.R., Cumming, B.F., 2000. Rainfall and drought in equatorial east Africa during the past 1,100 years. Nature 403, 410–414. https://doi.org/10.1038/35000179

von Höhnel, L., Rosiwal, A., Toula, F., Suess, E., 1891. Beiträge zur geologischen Kenntniss des östlichen Afrika (Contributions to the Geological Knowledge of Eastern Africa). Denkschriften der Akademie der Wissenshaften. Mathematisch-Naturwissenschaftlichen Klasse 58, 447–584.

Walumona, J.R., Kaunda-Arara, B., Odoli Ogombe, C., Murakaru, J.M., Raburu, P., Muvundja Amisi, F., Nyakeya, K., Kondowe, B.N., 2022. Effects of lake-level changes on water quality and fisheries production of Lake Baringo, Kenya. Ecohydrology 15. https://doi.org/10.1002/eco.2368

Wambui, P., Okeyo, F., Onywere, S., 2021. The Rift Valley Lakes Level Rise - Biophysical and Ecological Dilemma in Lake Baringo and Bogoria [WWW Document]. URL https://storymaps.arcgis.com/stories/60b7f2a46ba14775863b516f1edfe34a (accessed 2.16.23).

Wessel, B., 2018. TanDEM-X Ground Segment – DEM Products Specification Document TD-GS-PS-0021, Issue 3.2. Oberpfaffenhofen, Germany.

Whittaker, K.T., 2019. The Limnology, Climatology and Paleoclimatology of the East African Lakes, The Limnology, Climatology and Paleoclimatology of the East African Lakes. Routledge. https://doi.org/10.1201/9780203748978

Whittaker, K.T., Johnson, T.C., 2019. Sedimentary Processes and Signals of Past Climatic Change in the Large Lakes of the East African Rift Valley, in: The Limnology, Climatology and Paleoclimatology of the East African Lakes. Routledge, pp. 367–412. https://doi.org/10.1201/9780203748978-21

Wu, J., Yang, H., Yu, W., Yin, C., He, Y., Zhang, Z., Xu, D., Li, Q., Chen, J., 2022. Effect of Ecosystem Degradation on the Source of Particulate Organic Matter in a Karst Lake: A Case Study of the Caohai Lake, China. Water (Basel) 14, 1867. https://doi.org/10.3390/w14121867

Wuytack, T., Verschuren, D. (promotor), de Cort, G. (copromotor), van der Plas, G. (copromotor), 2017. Paleolimnological evidence for historical land use in the Lake Bogoria area of the central Rift Valley, Kenya. Ghent University & KU Leuven.

Yamazaki, D., Ikeshima, D., Sosa, J., Bates, P.D., Allen, G.H., Pavelsky, T.M., 2019. MERIT Hydro: A High-Resolution Global Hydrography Map Based on Latest Topography Dataset. Water Resour Res 55, 5053–5073. https://doi.org/10.1029/2019WR024873

Yao, J., Chen, Y., Zhao, Y., Yu, X., 2018. Hydroclimatic changes of Lake Bosten in Northwest China during the last decades. Sci Rep 8, 9118. https://doi.org/10.1038/s41598-018-27466-2

Yihdego, Y., Becht, R., 2013. Simulation of lake-aquifer interaction at Lake Naivasha, Kenya using a three-dimensional flow model with the high conductivity technique and a DEM with bathymetry. J Hydrol (Amst) 503, 111–122. https://doi.org/10.1016/j.jhydrol.2013.08.034

Zadereev, E., Lipka, O., Karimov, B., Krylenko, M., Elias, V., Pinto, I.S., Alizade, V., Anker, Y., Feest, A., Kuznetsova, D., Mader, A., Salimov, R., Fischer, M., 2020. Overview of past, current, and future ecosystem and biodiversity trends of inland saline lakes of Europe and Central Asia. Inland Waters 10, 438–452. https://doi.org/10.1080/20442041.2020.1772034

12 Appendix

12.1 Figures

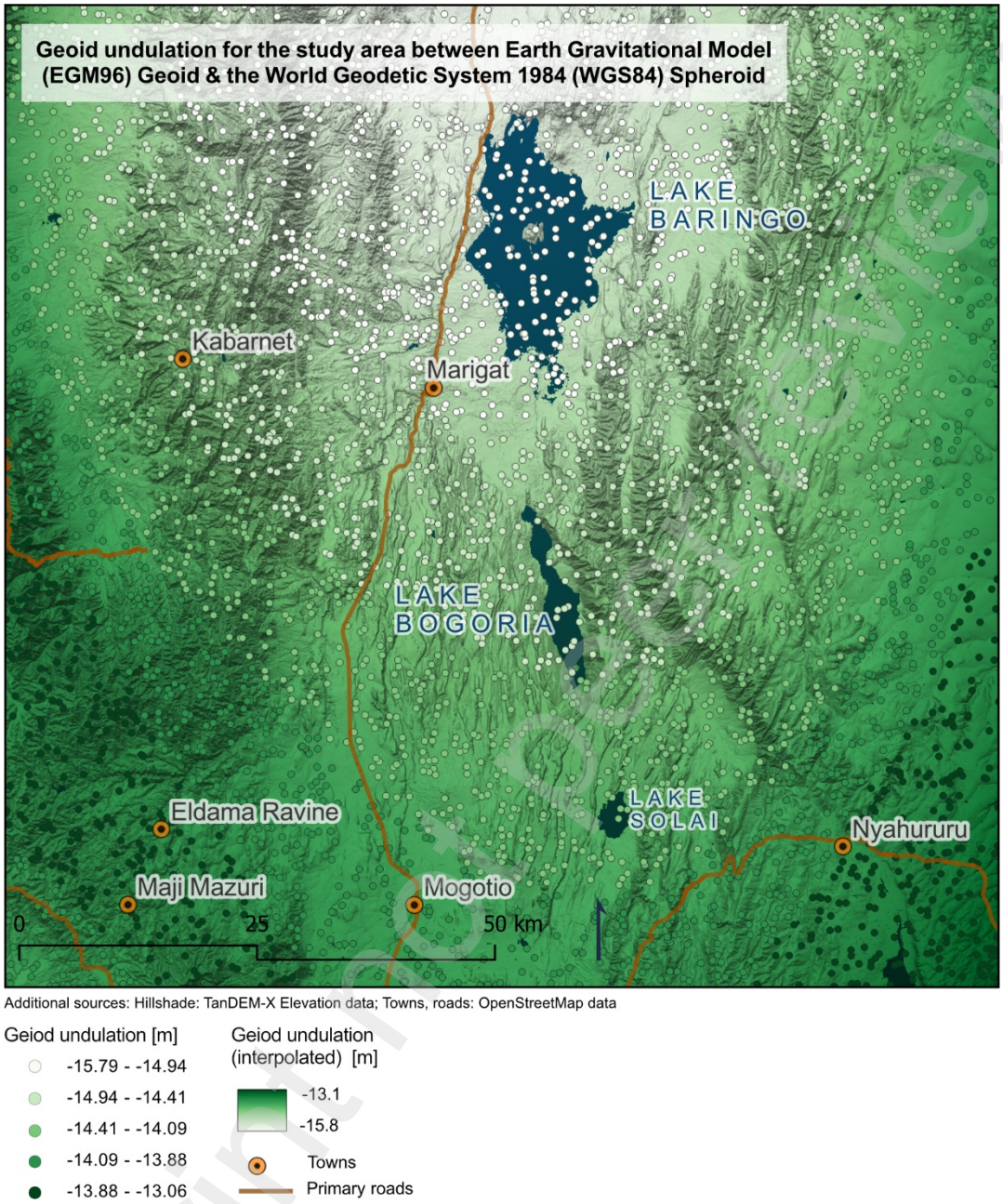

Figure A1: Geoid undulation for the study area. The interpolated elevation values are based on 5000 randomly sampled points, which are also shown.

Figure A2: Kiborkoch swamp in the proximity of the sill point of Lake Bogoria.

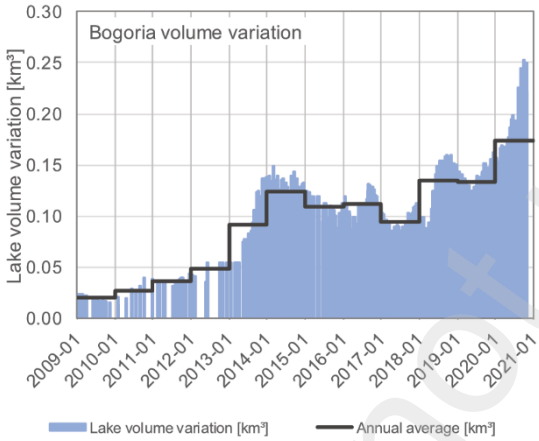

Figure A3: Lake Bogoria volume variation [km³], including annual averages.

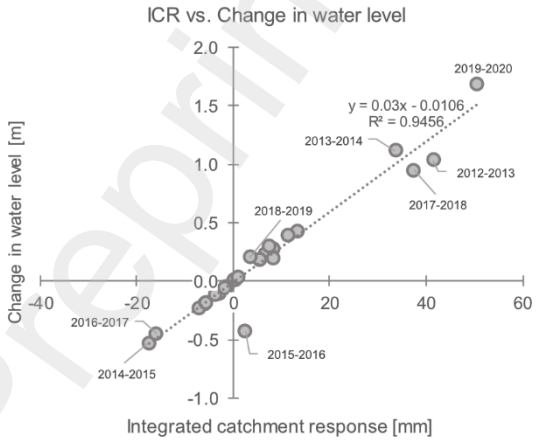

Figure A4: Relationship between Integrated catchment response and year to year change in water level for Lake Bogoria. The linear regression line with an R^2 of 0.95 is also shown.

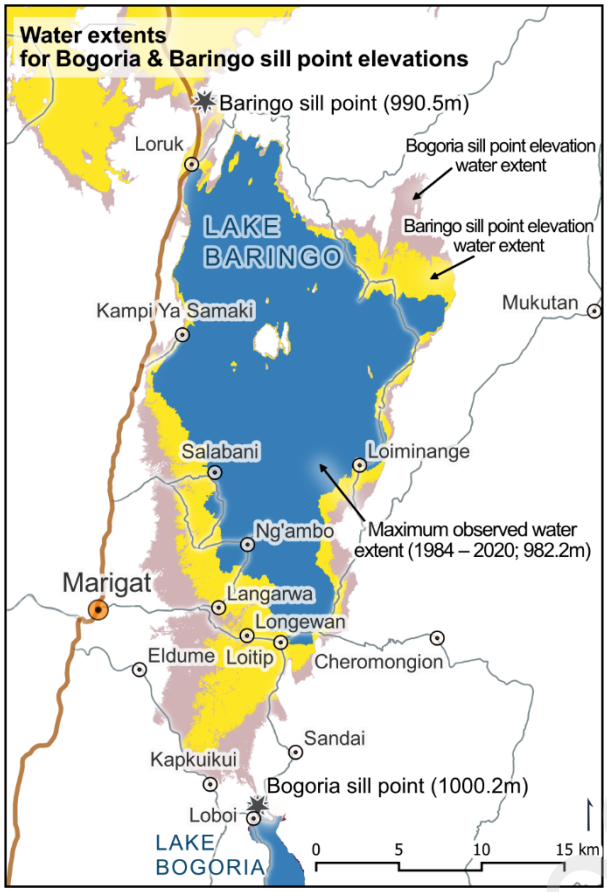

Figure A5: Water extents for Lake Bogoria and Lake Baringo sill point elevations. The water extent of the Lake Bogoria sill point elevation is hypothetical since the sill point elevation of Lake Baringo would be reached earlier and would overflow beforehand.

12.2 Tables

Table A1: Electrical conductivity and Temperature measurements

ID	Name	Type	EC [µS/cm]	Temperatur [°C]	Comment	Measurement date	Latitude [°]	Longitude [°]	SRTM elevation [masl]
1	Molo - Headwater	River	168.2	22.5		13.10.2022	0.0555	35.9673	1526.0
2	Rongai - D365 Bridge	River	308.8	27.6		13.10.2022	0.0625	35.9758	1529.0
3	Loboi - Headwater 1	River	NA	NA	River bed dry	13.10.2022	0.0992	36.0348	1478.0
4	Loboi - Headwater 2	River	NA	NA	River bed dry	13.10.2022	0.2820	36.0523	1138.0
5	Loboi - Maji Moto Hot Spring	Spring	552.4	34.8	Below spring	13.10.2022	0.2646	36.0454	1157.0
6	Loboi - downstream Maji Moto	River	588.1	29.9	River crossing (ford)	13.10.2022	0.2818	36.0523	1138.0
7	Chebaran 1	River	NA	NA	River dry, some pools with water, crocodiles	14.10.2022	0.4358	35.9994	1011.0
8	Small swamp Marigat-Loboi Road	Swamp	165.8	27.0		14.10.2022	0.4239	36.0090	1003.0
9	Perkerra River Discharge Gauging Station	River	113.5	23.3		14.10.2022	0.4589	35.9699	1073.0
10	Molo at Marigat-Loboi Road	River	171.5	24.0		14.10.2022	0.4374	36.0020	1012.0
11	Irrigation channel Marigat-Loboi Road	Irrigitation	172.4	24.0		14.10.2022	0.4218	36.0092	1002.0
12	Small stream out of swamp Marigat-Loboi Road	Stream	172.4	24.8	Flowing north	14.10.2022	0.3676	36.0449	1011.0
13	Spa Resort Spring Marigat-Loboi Road	Spring	646.0	36.1	River crossing (ford)	14.10.2022	0.3578	36.0512	1016.0
14	Loboi at Marigat-Loboi Road	River	1042.0	28.4	Under bridge	14.10.2022	0.3576	36.0579	1019.0
15	Stream from Spa Resort Spring	Stream	584.0	32.6	flowing north, natural, used for irrigation	14.10.2022	0.3651	36.0524	1009.0
16	Stream from Spa Resort Spring entering Loboi swamp	Stream	653.0	31.1		14.10.2022	0.3818	36.0501	996.0
17	Lake Bogoria	Lake	33800.0	34.7		14.10.2022	0.3507	36.0644	997.0
18	Loboi-Sandai Road culvert 1	Stream	1282.0	37.7	small stream flowing towards Bogoria	14.10.2022	0.3601	36.0664	1002.0
19	Loboi-Sandai Road culvert 2	Stream	1251.0	28.9	small stream flowing towards Bogoria	14.10.2022	0.3601	36.0670	1002.0
20	Sill point stream towards Lake Bogoria	Stream	1245.0	30.9	small stream flowing towards Bogoria	14.10.2022	0.3615	36.0669	1007.0
21	Kiborkoch Swamp (Sill point swamp) 0	Swamp	1247.0	29.7	stagnant water	14.10.2022	0.3634	36.0670	1006.0
22	Northern water line of sill point swamp	Swamp	813.0	27.7	stagnant water	14.10.2022	0.3714	36.0669	1007.0
23	Kiborkoch Swamp (Sill point swamp) 4	Swamp	958.0	31.0	stagnant water	14.10.2022	0.3709	36.0670	1005.0

ID	Name	Type	EC [µS/cm]	Temperatur [°C]	Comment	Measurement date	Latitude [°]	Longitude [°]	SRTM elevation [masl]
24	Kiborkoch Swamp (Sill point swamp) 3	Swamp	1218.0	25.0	stagnant water	14.10.2022	0.3700	36.0666	1007.0
25	Kiborkoch Swamp (Sill point swamp) 2	Swamp	1215.0	24.6	stagnant water	14.10.2022	0.3687	36.0665	1004.0
26	Kiborkoch Swamp (Sill point swamp) 1	Swamp	1220.0	27.0	stagnant water	14.10.2022	0.3676	36.0670	1004.0
27	Waseges / Sandai (Kesubo Swamp?)	River/Swamp	319.0	28.9	stagnant water	14.10.2022	0.3632	36.0724	1009.0
28	Waseges / Sandai (Discharge Station)	River	274.0	29.7	water flowing, irrigation diversion functioning	14.10.2022	0.3906	36.0898	1038.0
29	Lake 94	Swamp	581.0	36.2	stagnant water	14.10.2022	0.4572	36.0909	982.0
30	Ol Arabel River Branch	River	302.0	27.5	River crossing (ford)	14.10.2022	0.4825	36.1122	985.0
31	Ol Arabel	River	311.0	31.1	River crossing (ford)	14.10.2022	0.5128	36.1251	1016.0
32	Lake Baringo South at Loiminange	Lake	468.0	29.1		14.10.2022	0.5525	36.1214	982.0
34	Molo bridge - C51 road	River	210.0	28.4		14.10.2022	0.4631	36.0408	985.0
34a	Perkerra bridge	River	129.7	30.6	Bridge destroyed	14.10.2022	0.4631	36.0408	995.0
35	Tikirich River upstream	River	131.4	29.5		14.10.2022	0.4548	36.0499	996.0
36	Irrigation channel Eldume Kailer Road 1	Irrigation	207.0	23.9		15.10.2022	0.4239	36.0099	1007.0
37	Irrigiation channel Eldume Kailer Road 2	Irrigation	199.5	22.8		15.10.2022	0.4202	36.0147	1001.0
38	Perkerra main irrigation channel weir	Irrigitation	129.4	25.6		15.10.2022	0.4708	35.9980	1017.0
39	Stream between swamps	Stream	207.0	23.4		15.10.2022	0.4193	36.0135	1001.0
40	Loboi - Eldume Kailer road 1	Stream	1612.0	23.5		15.10.2022	0.4144	36.0428	991.0
41	Perkerra irrigation channel - Papaya field	Irrigation	129.9	25.6		15.10.2022	0.4687	36.0169	1006.0
42	Pekerra/Tikirich River Delta 1	River	139.7	28.9		15.10.2022	0.4951	36.0615	983.0
43	Pekerra/Tikirich River Delta 2	River	141.1	29.7		15.10.2022	0.5033	36.0607	978.0
44	Pekerra/Tikirich Delta Baringo shore 1	Lake/River	143.1	33.0		15.10.2022	0.5038	36.0584	983.0
45	Pekerra/Tikirich Delta Baringo shore 2	Lake/River	186.2	35.0		15.10.2022	0.5035	36.0584	983.0
46	L. Baringo - Kampi Ya Samaki - laundary washing site	Lake	491.0	33.6		15.10.2022	0.6209	36.0282	981.0
47	L. Baringo - Kampi Ya Samaki - Desert Rose Camp	Lake	473.0	32.0		15.10.2023	0.6222	36.0288	980.0
48	Loboi - Eldume Kailer road 2	Stream	1653.0	27.8		16.10.2022	0.4145	36.0428	991.0
49	Loboi - Eldume Kailer road 3	Stream	1618.0	24.8		16.10.2022	0.4145	36.0434	991.0

Table A2: Mean annual rainfall and number of days with intense rainfall ≥ 30 mm/d for Marigat (STN102)

Year	Marigat annual rainfall [mm/a]	Days with rainfall ≥ 30 mm/d
1986	373.8	0
1987	390.1	2
1988	616.3	3
1989	513.2	2
1990	336	0
1991	522.3	3
1992	233.5	0
1993	382.7	2
1994	542.7	5
1995	384.1	5
1996	542.7	5
1997	659.6	5
1998	430.6	3
1999	175.5	0
2000	211.5	0
2001	430.8	1
2002	274.7	1
2003	242.8	2
2004	267.7	2
2005	579.3	3
2006	516.3	2
2007	899.6	6

Year	Marigat annual rainfall [mm/a]	Days with rainfall ≥ 30 mm/d
2008	529.1	2
2009	1059.6	6
2010	1148.3	14
2011	1061.5	11
2012	899.5	11
2013	1654.5	16
2014	315.5	5
2015	708.2	8
2016	1250.7	14
2017	1059.4	11
2018	702.7	4

1360

Table A3: Mean annual lake volume variation and mean annual lake levels for Lake Bogoria based on DAHITI. Catchment rainfall based on CHIRPS. Values marked with an asterisk (*) are interpolated due to missing data.

Year	Mean annual lake volume variation [km³]	Mean annual lake level [m]	Lake Bogoria catchment rainfall [mm]
1984	0.008	993.3	541.8
1985	0.005*	993.2*	925.1
1986	0.002	993.1	936.9
1987	0.002	993.1	785.3
1988	0.009*	993.4*	1091.8
1989	0.016	993.6	1092.6
1990	0.013*	993.5*	957.1
1991	0.010*	993.4*	873.9

Year	Mean annual lake volume variation [km³]	Mean annual lake level [m]	Lake Bogoria catchment rainfall [mm]
1992	0.007	993.3	913.7
1993	0.007*	993.3*	840.7
1994	0.007	993.3	911.1
1995	0.006	993.3	954.5
1996	0.012*	993.4*	1012.6
1997	0.017*	993.6*	1248.2
1998	0.023*	993.8*	1126.5
1999	0.029	994.0	727.1
2000	0.023	993.8	707.1
2001	0.022	993.7	1162.7
2002	0.018	993.6	972.9
2003	0.016	993.6	1047.8
2004	0.017	993.6	934.2
2005	0.010	993.4	931.0
2006	0.003	993.2	1038.9
2007	0.017	993.6	1250.4
2008	0.025	993.9	848.6
2009	0.019	993.7	757.6
2010	0.027	994.0	1270.9
2011	0.036	994.2	1206.4
2012	0.048	994.6	1329.4
2013	0.092	995.6	1486.5
2014	0.128	996.7	882.4
2015	0.109	996.2	842.7
2016	0.112	995.8	970.2
2017	0.095	995.3	1159.5
2018	0.134	996.3	1554.9

Year	Mean annual lake volume variation [km³]	Mean annual lake level [m]	Lake Bogoria catchment rainfall [mm]
2019	0.138	996.5	1211.6
2020	0.192	998.1	1588.2
2021	NA	999.1	NA
2022	NA	998.4	NA

Table A4: Year to year changes in mean annual volume variation and water level and ICR. Values marked with an asterisk (*) are based on interpolated annual values.

Year	Year to year change in mean annual lake volume variation [km³]	ICR [mm]	Year to year change in Lake Bogoria water level [m]
1984-1985	-0.0033*	-3.1	-0.10*
1985-1986	-0.0033*	-3.1	-0.10*
1986-1987	0.0005	0.5	0.01
1987-1988	0.0070*	6.6	0.23*
1988-1989	0.0070*	6.6	0.23*
1989-1990	-0.0032	-3.0	-0.10*
1990-1991	-0.0032	-3.0	-0.10*
1991-1992	-0.0032	-3.0	-0.10*
1992-1993	0.0003	0.2	0.01*
1993-1994	0.0002	0.2	0.01
1994-1995	-0.0013	-1.3	-0.04
1995-1996	0.0058*	5.5	0.18*
1996-1997	0.0058*	5.5	0.18*
1997-1998	0.0058*	5.5	0.18*

Year	Year to year change in mean annual lake volume variation [km³]	ICR [mm]	Year to year change in Lake Bogoria water level [m]
1998-1999	0.0058*	5.5	0.18*
1999-2000	-0.0060	-5.7	-0.19
2000-2001	-0.0015	-1.4	-0.04
2001-2002	-0.0039	-3.7	-0.12
2002-2003	-0.0020	-1.9	-0.06
2003-2004	0.0010	1.0	0.03
2004-2005	-0.0065	-6.1	-0.20
2005-2006	-0.0075	-7.1	-0.24
2006-2007	0.0139	13.2	0.43
2007-2008	0.0089	8.4	0.27
2008-2009	-0.0061	-5.7	-0.18
2009-2010	0.0080	7.5	0.30
2010-2011	0.0089	8.4	0.20
2011-2012	0.0119	11.2	0.39
2012-2013	0.0439	41.4	1.03
2013-2014	0.0356	33.6	1.12
2014-2015	-0.0185	- 17.5	-0.53
2015-2016	0.0026	2.5	-0.42
2016-2017	-0.0170	- 16.0	-0.45
2017-2018	0.0397	37.4	0.95
2018-2019	0.0037	3.5	0.20
2019-2020	0.0536	50.6	1.69
2020-2021	NA	NA	0.94

Year	Year to year change in mean annual lake volume variation [km³]	ICR [mm]	Year to year change in Lake Bogoria water level [m]
2021-2022	NA	NA	-0.72
2022-2023	NA	NA	-0.41

1365

Table A5: Calculation of empirical probability to reach sill point with maximum observed water level 1984–2020 as initial Lake Bogoria water level (0.70 m to reach sill point elevation). Year-to-year change in water level values marked with an asterisk (*) are based on interpolated annual values of water level.

Empirical probability - Maximum observed water level 1984–2020 as initial value (0.70 m to reach sill point elevation)										
Year	Year-to-year change in water level [m]	Occurrence (yes/no) (1 years)	Cumulative year-to-year change in water level [m] (2 years)	Occurrence (yes/no) (2 years)	Cumulative year-to-year change in water level [m] (3 years)	Occurrence (yes/no) (5 years)	Cumulative year-to-year change in water level [m] (4 years)	Occurrence (yes/no) (5 years)	Cumulative year-to-year change in water level [m] (5 years)	Occurrence (yes/no) (5 years)
1984-1985	-0.10*	0								
1985-1986	-0.10*	0	-0.20	0						
1986-1987	0.01	0	-0.09	0	-0.19	0				
1987-1988	0.23*	0	0.24	0	0.14	0	0.04	0		
1988-1989	0.23*	0	0.45	0	0.46	0	0.36	0	0.26	0
1989-1990	-0.10*	0	0.12	0	0.35	0	0.36	0	0.26	0
1990-1991	-0.10*	0	-0.20	0	0.02	0	0.25	0	0.26	0
1991-1992	-0.10*	0	-0.20	0	-0.30	0	-0.08	0	0.15	0
1992-1993	0.01*	0	-0.09	0	-0.20	0	-0.30	0	-0.07	0
1993-1994	0.01	0	0.01	0	-0.09	0	-0.19	0	-0.29	0
1994-1995	-0.04	0	-0.04	0	-0.03	0	-0.13	0	-0.23	0

Empirical probability - Maximum observed water level 1984–2020 as initial value (0.70 m to reach sill point elevation)										
Year	Year-to-year change in water level [m]	Occurrence (yes/no) (1 years)	Cumulative year-to-year change in water level [m] (2 years)	Occurrence (yes/no) (2 years)	Cumulative year-to-year change in water level [m] (3 years)	Occurrence (yes/no) (5 years)	Cumulative year-to-year change in water level [m] (4 years)	Occurrence (yes/no) (5 years)	Cumulative year-to-year change in water level [m] (5 years)	Occurrence (yes/no) (5 years)
1995-1996	0.18*	0	0.14	0	0.14	0	0.15	0	0.05	0
1996-1997	0.18*	0	0.36	0	0.31	0	0.32	0	0.33	0
1997-1998	0.18*	0	0.36	0	0.54	0	0.49	0	0.50	0
1998-1999	0.18*	0	0.36	0	0.54	0	0.72	1	0.67	0
1999-2000	-0.19	0	-0.01	0	0.17	0	0.35	0	0.53	0
2000-2001	-0.04	0	-0.23	0	-0.05	0	0.13	0	0.31	0
2001-2002	-0.12	0	-0.16	0	-0.35	0	-0.17	0	0.01	0
2002-2003	-0.06	0	-0.18	0	-0.22	0	-0.41	0	-0.23	0
2003-2004	0.03	0	-0.03	0	-0.15	0	-0.19	0	-0.38	0
2004-2005	-0.20	0	-0.17	0	-0.23	0	-0.35	0	-0.39	0
2005-2006	-0.24	0	-0.44	0	-0.41	0	-0.47	0	-0.59	0
2006-2007	0.43	0	0.19	0	-0.01	0	0.02	0	-0.04	0
2007-2008	0.27	0	0.70	1	0.47	0	0.27	0	0.30	0
2008-2009	-0.18	0	0.09	0	0.52	0	0.29	0	0.08	0
2009-2010	0.30	0	0.12	0	0.39	0	0.82	1	0.58	0
2010-2011	0.20	0	0.50	0	0.31	0	0.59	0	1.02	1
2011-2012	0.39	0	0.59	0	0.89	1	0.71	1	0.98	1
2012-2013	1.03	1	1.42	1	1.62	1	1.92	1	1.74	1

Empirical probability - Maximum observed water level 1984–2020 as initial value (0.70 m to reach sill point elevation)										
Year	**Year-to-year change in water level [m]**	**Occurrence (yes/no) (1 years)**	**Cumulative year-to-year change in water level [m] (2 years)**	**Occurrence (yes/no) (2 years)**	**Cumulative year-to-year change in water level [m] (3 years)**	**Occurrence (yes/no) (5 years)**	**Cumulative year-to-year change in water level [m] (4 years)**	**Occurrence (yes/no) (5 years)**	**Cumulative year-to-year change in water level [m] (5 years)**	**Occurrence (yes/no) (5 years)**
2013-2014	1.12	1	2.15	1	2.54	1	2.74	1	3.04	1
2014-2015	-0.53	0	0.59	0	1.62	1	2.01	1	2.21	1
2015-2016	-0.42	0	-0.95	0	0.16	0	1.20	1	1.59	1
2016-2017	-0.45	0	-0.87	0	-1.40	0	-0.29	0	0.75	1
2017-2018	0.95	1	0.50	0	0.08	0	-0.45	0	0.66	0
2018-2019	0.20	0	1.15	1	0.70	1	0.28	0	-0.25	0
2019-2020	1.69	1	1.89	1	2.84	1	2.39	1	1.97	1
2020-2021	0.94	1	2.63	1	2.83	1	3.78	1	3.34	1
2021-2022	-0.72	0	0.23	0	1.92	1	2.12	1	3.07	1
Empirical probability to reach sill point (Climate 2009-2022 (wet))		**38.5%**		**38.5%**		**61.5%**		**69.2%**		**76.9%**
Empirical probability to reach sill point (Climate 1984–2022 (long-term))		**13.2%**		**16.2%**		**22.2%**		**28.6%**		**29.4%**

Table A6: Calculation of empirical probability to reach sill point with water level of February 2023 as initial Lake Bogoria water level (2.2 m to reach sill point elevation). Year-to-year change in water level values marked with an asterisk (*) are based on interpolated annual values of water level.

Empirical probability - water level of Feb. 2023 as initial value (2.2 m to reach sill point elevation)										
Year	**Year-to-year change in water level [m]**	**Occurrence (yes/no) (1 years)**	**Cumulative year-to-year change in water level [m] (2 years)**	**Occurrence (yes/no) (2 years)**	**Cumulative year-to-year change in water level [m] (3 years)**	**Occurrence (yes/no) (5 years)**	**Cumulative year-to-year change in water level [m] (4 years)**	**Occurrence (yes/no) (5 years)**	**Cumulative year-to-year change in water level [m] (5 years)**	**Occurrence (yes/no) (5 years)**
1984-1985	-0.10*	0								
1985-1986	-0.10*	0	-0.20	0						
1986-1987	0.01	0	-0.09	0	-0.19	0				
1987-1988	0.23*	0	0.24	0	0.14	0	0.04	0		
1988-1989	0.23*	0	0.45	0	0.46	0	0.36	0	0.26	0
1989-1990	-0.10*	0	0.12	0	0.35	0	0.36	0	0.26	0
1990-1991	-0.10*	0	-0.20	0	0.02	0	0.25	0	0.26	0
1991-1992	-0.10*	0	-0.20	0	-0.30	0	-0.08	0	0.15	0
1992-1993	0.01*	0	-0.09	0	-0.20	0	-0.30	0	-0.07	0
1993-1994	0.01	0	0.01	0	-0.09	0	-0.19	0	-0.29	0
1994-1995	-0.04	0	-0.04	0	-0.03	0	-0.13	0	-0.23	0
1995-1996	0.18*	0	0.14	0	0.14	0	0.15	0	0.05	0
1996-1997	0.18*	0	0.36	0	0.31	0	0.32	0	0.33	0
1997-1998	0.18*	0	0.36	0	0.54	0	0.49	0	0.50	0
1998-1999	0.18*	0	0.36	0	0.54	0	0.72	0	0.67	0
1999-2000	-0.19	0	-0.01	0	0.17	0	0.35	0	0.53	0
2000-2001	-0.04	0	-0.23	0	-0.05	0	0.13	0	0.31	0

Empirical probability - water level of Feb. 2023 as initial value (2.2 m to reach sill point elevation)										
Year	Year-to-year change in water level [m]	Occurrence (yes/no) (1 years)	Cumulative year-to-year change in water level [m] (2 years)	Occurrence (yes/no) (2 years)	Cumulative year-to-year change in water level [m] (3 years)	Occurrence (yes/no) (5 years)	Cumulative year-to-year change in water level [m] (4 years)	Occurrence (yes/no) (5 years)	Cumulative year-to-year change in water level [m] (5 years)	Occurrence (yes/no) (5 years)
2001-2002	-0.12	0	-0.16	0	-0.35	0	-0.17	0	0.01	0
2002-2003	-0.06	0	-0.18	0	-0.22	0	-0.41	0	-0.23	0
2003-2004	0.03	0	-0.03	0	-0.15	0	-0.19	0	-0.38	0
2004-2005	-0.20	0	-0.17	0	-0.23	0	-0.35	0	-0.39	0
2005-2006	-0.24	0	-0.44	0	-0.41	0	-0.47	0	-0.59	0
2006-2007	0.43	0	0.19	0	-0.01	0	0.02	0	-0.04	0
2007-2008	0.27	0	0.70	0	0.47	0	0.27	0	0.30	0
2008-2009	-0.18	0	0.09	0	0.52	0	0.29	0	0.08	0
2009-2010	0.30	0	0.12	0	0.39	0	0.82	0	0.58	0
2010-2011	0.20	0	0.50	0	0.31	0	0.59	0	1.02	0
2011-2012	0.39	0	0.59	0	0.89	0	0.71	0	0.98	0
2012-2013	1.03	0	1.42	0	1.62	0	1.92	0	1.74	0
2013-2014	1.12	0	2.15	0	2.54	1	2.74	1	3.04	1
2014-2015	-0.53	0	0.59	0	1.62	0	2.01	0	2.21	1
2015-2016	-0.42	0	-0.95	0	0.16	0	1.20	0	1.59	0
2016-2017	-0.45	0	-0.87	0	-1.40	0	-0.29	0	0.75	0
2017-2018	0.95	0	0.50	0	0.08	0	-0.45	0	0.66	0
2018-2019	0.20	0	1.15	0	0.70	0	0.28	0	-0.25	0

Empirical probability - water level of Feb. 2023 as initial value (2.2 m to reach sill point elevation)										
Year	**Year-to-year change in water level [m]**	**Occurrence (yes/no) (1 years)**	**Cumulative year-to-year change in water level [m] (2 years)**	**Occurrence (yes/no) (2 years)**	**Cumulative year-to-year change in water level [m] (3 years)**	**Occurrence (yes/no) (5 years)**	**Cumulative year-to-year change in water level [m] (4 years)**	**Occurrence (yes/no) (5 years)**	**Cumulative year-to-year change in water level [m] (5 years)**	**Occurrence (yes/no) (5 years)**
2019-2020	1.69	0	1.89	0	2.84	1	2.39	1	1.97	0
2020-2021	0.94	0	2.63	1	2.83	1	3.78	1	3.34	1
2021-2022	-0.72	0	0.23	0	1.92	0	2.12	0	3.07	1
Empirical probability to reach sill point (Climate 2009-2022 (wet))		**0.0%**		**7.7%**		**23.1%**		**23.1%**		**30.8%**
Empirical probability to reach sill point (Climate 1984–2022 (long-term))		**0.0%**		**2.7%**		**8.3%**		**8.6%**		**11.8%**